

E3-1788

2

AD-A159 280

DNA-TR-84-272

FIRE DAMAGE AND STRATEGIC TARGETING

**Harold L. Brode
Richard D. Small
Pacific-Sierra Research Corporation
12340 Santa Monica Boulevard
Los Angeles, CA 90025-2587**

1 June 1984

Technical Report

CONTRACT No. DNA 001-82-C-0046

**Approved for public release;
distribution is unlimited.**

DTIC FILE COPY

**THIS WORK WAS SPONSORED BY THE DEFENSE NUCLEAR AGENCY
UNDER RDT&E RMSS CODE B384082466 V99QAXNL00084 H2590D.**

**Prepared for
Director
DEFENSE NUCLEAR AGENCY
Washington, DC 20305-1000**

**DTIC FILE COPY
SEP 20 1985**

85 7 17 028

Destroy this report when it is no longer needed. Do not return to sender.

PLEASE NOTIFY THE DEFENSE NUCLEAR AGENCY, ATTN: STTI, WASHINGTON, DC 20305-1000, IF YOUR ADDRESS IS INCORRECT, IF YOU WISH IT DELETED FROM THE DISTRIBUTION LIST, OR IF THE ADDRESSEE IS NO LONGER EMPLOYED BY YOUR ORGANIZATION.

Assignment For	
S GRA&I	<input checked="" type="checkbox"/>
C TAB	<input type="checkbox"/>
announced	<input type="checkbox"/>
ification	<input type="checkbox"/>
Distribution/	
Availability Codes	
Dist	Special
A-1	



UNCLASSIFIED

AD-A159280

SECURITY CLASSIFICATION OF THIS PAGE

REPORT DOCUMENTATION PAGE

1a REPORT SECURITY CLASSIFICATION UNCLASSIFIED			1b RESTRICTIVE MARKINGS			
2a SECURITY CLASSIFICATION AUTHORITY			3 DISTRIBUTION / AVAILABILITY OF REPORT Approved for public release; distribution is unlimited.			
2b DECLASSIFICATION / DOWNGRADING SCHEDULE N/A since UNCLASSIFIED			5 MONITORING ORGANIZATION REPORT NUMBER(S) DNA-TR-84-272			
4 PERFORMING ORGANIZATION REPORT NUMBER(S)			7a NAME OF MONITORING ORGANIZATION Director Defense Nuclear Agency			
6a NAME OF PERFORMING ORGANIZATION Pacific-Sierra Research Corporation		6b OFFICE SYMBOL (If applicable)		7b ADDRESS (City, State and ZIP Code) Washington, DC 20305-1000		
6c ADDRESS (City, State, and ZIP Code) 12340 Santa Monica Boulevard Los Angeles, CA 90025-2587			8a NAME OF FUNDING / SPONSORING ORGANIZATION			
8b OFFICE SYMBOL (If applicable)		9 PROCUREMENT INSTRUMENT IDENTIFICATION NUMBER DNA 001-82-C-0046				
8c ADDRESS (City, State, and ZIP Code)			10 SOURCE OF FUNDING NUMBERS			
			PROGRAM ELEMENT NO 62715H	PROJECT NO V99QAXN	TASK NO L	WORK UNIT ACCESSION NO DHQ05685
11 TITLE (Include Security Classification) FIRE DAMAGE AND STRATEGIC TARGETING						
12 PERSONAL AUTHOR(S) Harold L. Brode, Richard D. Small						
13a TYPE OF REPORT Technical Report		13b TIME COVERED FROM 820501 TO 830630		14 DATE OF REPORT (Year Month Day) 1984, June 1		15 PAGE COUNT 52
16 SUPPLEMENTARY NOTATION This work was sponsored by the Defense Nuclear Agency under RDT&E RMSS Code B384082466 V99QAXNLO0084 H2590D.						
17 COSATI CODES			18 SUBJECT TERMS (Continue on reverse if necessary and identify by block number)			
FIELD	GROUP	SUB-GROUP	Fires Blast Damage			
13	12		Fire Damage Civil Defense			
8	6		Urban Areas Thermal Radiation			
19 ABSTRACT (Continue on reverse if necessary and identify by block number) This report relates the probability of fire damage to blast-induced ignitions and those due to thermal radiation. Modifying influences such as weather conditions, target structure, and countermeasures are included. Since fires continue to develop long after the explosion, additional effects such as fire spread and fire-wind damage are also considered. The methods may be extended to calculate probable damage ranges for a specific target, and may be made compatible with current targeting algorithms (the DIA vulnerability number methodology).						
20 DISTRIBUTION / AVAILABILITY OF ABSTRACT <input type="checkbox"/> UNCLASSIFIED/UNLIMITED <input checked="" type="checkbox"/> SAME AS RPT <input type="checkbox"/> DTIC USERS			21 ABSTRACT SECURITY CLASSIFICATION UNCLASSIFIED			
22a NAME OF RESPONSIBLE INDIVIDUAL Betty L. Fox			22b TELEPHONE (Include Area Code) (202) 325-7042		22c OFFICE SYMBOL DNA/STTI	

DD FORM 1473, 84 MAR

83 APR edition may be used until exhausted
All other editions are obsolete

SECURITY CLASSIFICATION OF THIS PAGE

UNCLASSIFIED

SUMMARY

The blast wave and the thermal, electromagnetic, and nuclear radiations from a nuclear explosion can all contribute to target damage. Current strategic targeting considers structural damage from the blast wave only. Although fire damage can be more intensive and occur at greater ranges, it is treated as a bonus effect and thus not included in targeting or damage assessments. Since the variables controlling fire damage have been considered too uncertain to allow reliable fire damage predictions, there has been little impetus to modify targeting strategies to account for this added effect.

This report relates the probability of fire damage to blast-induced ignitions and those due to thermal radiation. Modifying influences such as weather conditions, target structure, and countermeasures are included. Since fires continue to develop long after the explosion, additional effects such as fire spread and fire-wind damage are also considered. The methods may be extended to calculate probable damage ranges for a specific target, and may be made compatible with current targeting algorithms (the DIA vulnerability number methodology).

"Reasonable" parameter values lead to fire damage ranges that extend into low overpressure regions. Less conservative--though still reasonable--values result in damage ranges exceeding comparable blast damage ranges. These results could help justify enlarging the scope of current targeting strategies to include fire effects. This study identifies those aspects of urban fires from nuclear attack that are most influential in determining the extent of fire damage and are still uncertain. These factors are proper candidates for further Defense Nuclear Agency research.

PREFACE

This report is one of a 16 volume set comprising the Pacific-Sierra Research Corporation (PSR) final report on Defense Nuclear Agency (DNA) contract DNA 001-82-C-0046. The work done under this contract spans a wide range of nuclear weapon effect research covering airblast, cratering and ground motion, low-dose radiation, underground test design and development, fire research, and electromagnetic pulse research. The contract technical monitor was Cyrus P. Knowles.

In a recent effort for DNA, H. L. Brode and R. D. Small of PSR cooperated with R. Port and E. Carson of R & D Associates (RDA) in a study to examine the potential role of fire in urban/industrial area targeting. The intent of this exercise was to explore the possible consequences of including fire damage in targeting and damage assessments and to illuminate those aspects of fire prediction that are both most uncertain and most important. This study would hopefully aid in guiding fire research.

The results were briefed to DNA, and included in reports to the JSTPS Scientific Advisory Group. This report summarizes the fire phenomenology contributions made by PSR. The targeting exercises (by RDA), using these PSR inputs, and our joint results and conclusions will be reported separately. The recent death of R. Port will make the completion and summarization of the targeting effects exceedingly difficult.

This task was supervised by Michael J. Frankel.

TABLE OF CONTENTS

<u>Section</u>	<u>Page</u>
SUMMARY	1
PREFACE	2
LIST OF ILLUSTRATIONS	4
1 INTRODUCTION	7
2 FIRE-DAMAGE-RANGE CURVES	9
3 THERMAL-RADIATION-INDUCED IGNITIONS	10
4 BLAST-INDUCED IGNITIONS	23
5 INITIAL FIRE STARTS--COMBINED IGNITION DISTRIBUTION	27
6 FIRE SPREAD	29
7 CIVIL DEFENSE	32
8 COMBINED-PARAMETER VARIATIONS	35
9 CONCLUSIONS	43
REFERENCES	45

LIST OF ILLUSTRATIONS

<u>Figure</u>	<u>Page</u>
1	Standard forms for calculating total visible radiation transmissivity from airbursts 11
2	Fire damage range for thermally induced ignitions: variable visibility lengths, $W = 50$ KT, $\alpha = 2.0$, $\beta = 1.4$ 14
3	Fire damage range for thermally induced ignitions: variable visibility lengths, $W = 50$ KT, $\alpha = 2.9$, $\beta = 1.9$ 14
4	Fire damage range for thermally induced ignitions: variable visibility lengths, $W = 1$ MT, $\alpha = 2.0$, $\beta = 1.4$ 15
5	Fire damage range for thermally induced ignitions: variable visibility lengths, $W = 1$ MT, $\alpha = 2.9$, $\beta = 1.9$ 15
6	Fire damage range for thermally induced ignitions: variable levels of radiation enhancement, $W = 50$ KT, $V = 12$ mi, $\alpha = 2.0$, $\beta = 1.4$ 17
7	Fire damage range for thermally induced ignitions: variable levels of radiation enhancement, $W = 1$ MT, $V = 12$ mi, $\alpha = 2.0$, $\beta = 1.4$ 17
8	Fire damage range for thermally induced ignitions: variable levels of radiation attenuation, $W = 50$ KT, $V = 12$ mi, $\alpha = 2.0$, $\beta = 1.4$ 18
9	Fire damage range for thermally induced ignitions: variable levels of radiation attenuation, $W = 1$ MT, $V = 12$ mi, $\alpha = 2.0$, $\beta = 1.4$ 18
10	Fire damage range for thermally induced ignitions: variable ignition threshold levels, $W = 50$ KT, $V = 12$ mi, $\alpha = 2.0$, $\beta = 1.4$ 20
11	Fire damage range for thermally induced ignitions: variable ignition threshold levels, $W = 1$ MT, $V = 12$ mi, $\alpha = 2.0$, $\beta = 1.4$ 20
12	Fire damage range for thermally induced ignitions: variable ignition threshold levels, $W = 50$ KT, $V = 12$ mi, $\alpha = 2.9$, $\beta = 1.9$ 21
13	Fire damage range for thermally induced ignitions: variable ignition threshold levels, $W = 1$ MT, $V = 12$ mi, $\alpha = 2.9$, $\beta = 1.9$ 21

LIST OF ILLUSTRATIONS (Continued)

<u>Figure</u>		<u>Page</u>
14	Fire damage range for blast-induced ignitions: variable building type/contents indices, W = 50 KT	26
15	Fire damage range for blast-induced ignitions: variable building type/contents indices, W = 1 MT	26
16	Fire damage range for thermally and blast-induced ignitions: variable levels of radiation attenuation and enhancement, W = 50 KT, V = 12 mi, $\alpha = 2.0$, $\beta = 1.4$, building type/contents index = 4/7.5	28
17	Fire damage range for thermally and blast-induced ignitions: variable levels of radiation attenuation and enhancement, W = 1 MT, V = 12 mi, $\alpha = 2.0$, $\beta = 1.4$, building type/contents index = 4/7.5	28
18	Fire damage range for thermally and blast-induced ignitions and fire spread: variable levels of radiation attenuation and enhancement, W = 50 KT, V = 12 mi, $\alpha = 2.0$, $\beta = 1.4$, building type/contents index = 4/7.5 ..	31
19	Fire damage range for thermally and blast-induced ignitions and fire spread: variable levels of radiation attenuation and enhancement, W = 1 MT, V = 12 mi, $\alpha = 2.0$, $\beta = 1.4$, building type/contents index = 4/7.5 ..	31
20	Fire damage range for various combinations of fire starts and spread with and without countermeasures: W = 50 KT, V = 12 mi, $\alpha = 2.0$, $\beta = 1.4$, building type/contents index = 4/7.5	33
21	Fire damage range for various combinations of fire starts and spread with and without countermeasures: W = 1 MT, V = 12 mi, $\alpha = 2.0$, $\beta = 1.4$, building type/contents index = 4/7.5	33
22	Fire damage range for thermally induced ignitions: combined-parameter variations with and without countermeasures, W = 50 KT	39
23	Fire damage range for thermally induced ignitions: combined-parameter variations with and without countermeasures, W = 1 MT	39
24	Fire damage range for blast-induced ignitions: combined-parameter variations with and without countermeasures, W = 50 KT	40

LIST OF ILLUSTRATIONS (Concluded)

<u>Figure</u>		<u>Page</u>
25	Fire damage range for blast-induced ignitions: combined-parameter variations with and without countermeasures, W = 1 MT	40
26	Fire damage range summation curves: all parameters, W = 50 KT	41
27	Fire damage range summation curves: all parameters, W = 1 MT	41

SECTION 1

INTRODUCTION

A nuclear weapon explosion will cause extensive blast damage and ignite many fires. Though damage radii characterizing probable blast destruction have been defined, comparable methods to estimate fire damage radii have not been developed. In view of the widespread and uniform fire damage observed at Hiroshima and Nagasaki, consideration of blast damage alone may underestimate the potential destruction from a nuclear weapon explosion.

There are several reasons why fires have been considered a bonus effect rather than a principal damage agent. Historically, fire has been viewed as largely unpredictable and too subject to the vagaries of weather and the errors in weapon delivery to be a reliable damage mechanism. Despite the uncertainties, World War II planners pursued a program of fire bombing raids. In many cases, damage was less than expected but still greater than could be achieved with general-purpose (explosive) bombs. In others, large conflagrations developed, and damage far exceeded predictions. As the war progressed, attacks on urban/industrial concentrations relied on fire bombing as the most effective damage mechanism.

A nuclear weapon is the modern analog to the raids by a thousand aircraft carrying mixes of thermite and high-explosive bombs. The concentration of the fire-causative mechanisms in a single nuclear warhead ensures a very large number of ignitions and the rapid development of a large area fire. Weather and other conventional modifying influences on small fires may be less important or reasonably predictable effects for large fires with multitudinous ignition sources. As a consequence, it may be reasonable to reconsider the inclusion of fire effects in target damage assessments.

The analysis in this report employs broad assumptions about large urban fires in order to provide inputs to a targeting study. A general relation is hypothesized to define fire damage as a function of range

for an urban area. The sensitivity of each parameter is evaluated by varying its values and noting its influence on the fire distribution. Some additional parameters not explicitly explored in the model are identified and discussed.

The principal parameters considered here are weapon yield, height of burst, threshold ignition levels, visibility length, atmospheric transmissivity, enhancement and attenuation of the thermal radiation due to clouds and snow cover, blast-induced ignitions as a function of building type and contents, fire spread, fire winds, and countermeasures. Following a systematic variation of each parameter, combinations of effects as well as combined expected deviations are considered. The results identify the sensitivity of each variable and its relative importance to the damage-range relation. Simultaneous variation of the group of parameters provides some insight into the likely overall uncertainty in fire damage predictions.

An alternative fire damage methodology for strategic targeting applications might supplement the current vulnerability number (VN) system with designations representing potential fire damage to each specified target. Such an expanded VN system has not yet been developed, but the elements for its creation are included here.

SECTION 2

FIRE-DAMAGE-RANGE CURVES

The fire-damage radius is related to two ignition mechanisms--the thermal radiation and the blast wave. In addition, the many initial fires will spread to nearby structures and to areas beyond the initial ignitions. Furthermore, the resulting large area fire may generate winds of hurricane force that can cause destruction beyond the fire perimeter.

The analysis used here relates target damage to the causative mechanisms in the following way. First, a target susceptibility to fire damage is estimated for both thermally and blast-induced ignitions. The vulnerability is expressed as an incident radiation flux level or as an overpressure, and thus related to the weapon yield and range. Other factors such as weather conditions, visibility length, transmissivity, cloud reflections or absorptions, and snow cover modify the damage-range relation. The two ignition mechanisms are assumed independent, and the resulting fire probabilities are combined to form a single damage-range curve representing the immediate weapon effects-target interaction. This result is then modified to account for fire spread and wind damage.

Identifying a target's susceptibility to fire damage and then determining a range consistent with that vulnerability parallels the procedure used to calculate blast damage ranges. The VN designator system facilitates the blast damage calculations. Although a similar procedure has not yet been fully developed to estimate vulnerabilities to fire as a function of building type, damage probabilities may be inferred from theoretical models, from measurements of ignition thresholds, and from analysis of the two nuclear-bombed Japanese cities. The uncertainties in the parameters are expressed as standard deviations about a mean damage-range curve.

SECTION 3

THERMAL-RADIATION-INDUCED IGNITIONS

More than a third of the total weapon energy is emitted as thermal radiation. The rapid deposition of this energy on combustible materials such as interior furnishings and flammable construction materials can start a large number of building fires. Those fires usually develop from interior ignitions that "flash over" to involve whole rooms either immediately or in approximately 15 to 30 min. In the nuclear case, there is the possibility of immediate flashover because of the massive thermal influx. In either case, the probability of fire damage is a function of the incident thermal flux, the level of blast effects, and the target susceptibility to thermal ignitions or blast disruption fires.

The thermal energy emitted is partially scattered and absorbed in the atmosphere between the fireball and the target. The amount arriving at a slant range (miles) is approximated for an airburst [Gibbons, 1966; DNA EM-1(N), 1974; Glasstone and Dolan, 1977; Martin and Alger, 1981] by the following:

$$Q = \frac{W}{\tilde{R}^2} \left(1 + \beta \frac{\tilde{R}}{V} \right) \exp \left(- \alpha \frac{\tilde{R}}{V} \right), \quad (1)$$

where W is the weapon yield in kilotons and V the local visibility length in miles.

This functional form is consistent with both weapon test data and theoretical radiation-hydrodynamic solutions, provided varying values of the absorption (α) and scattering (β) coefficients are used. Recommended values range from $\alpha, \beta = 2.9, 1.9$ [DNA EM-1(N), 1974] to $\alpha, \beta = 2.0, 1.4$ [Brode, 1964; Glasstone and Dolan, 1977]. Figure 1 compares the different forms. The differences are significant for moderate visibility lengths (\tilde{R}/V) or for low visibilities (small values of V). Urban atmospheres may be composed of different types of scattering centers or absorbing particles and thus may exhibit such a range of extinction coefficients (α) and scattering enhancements (β). The evidence is not

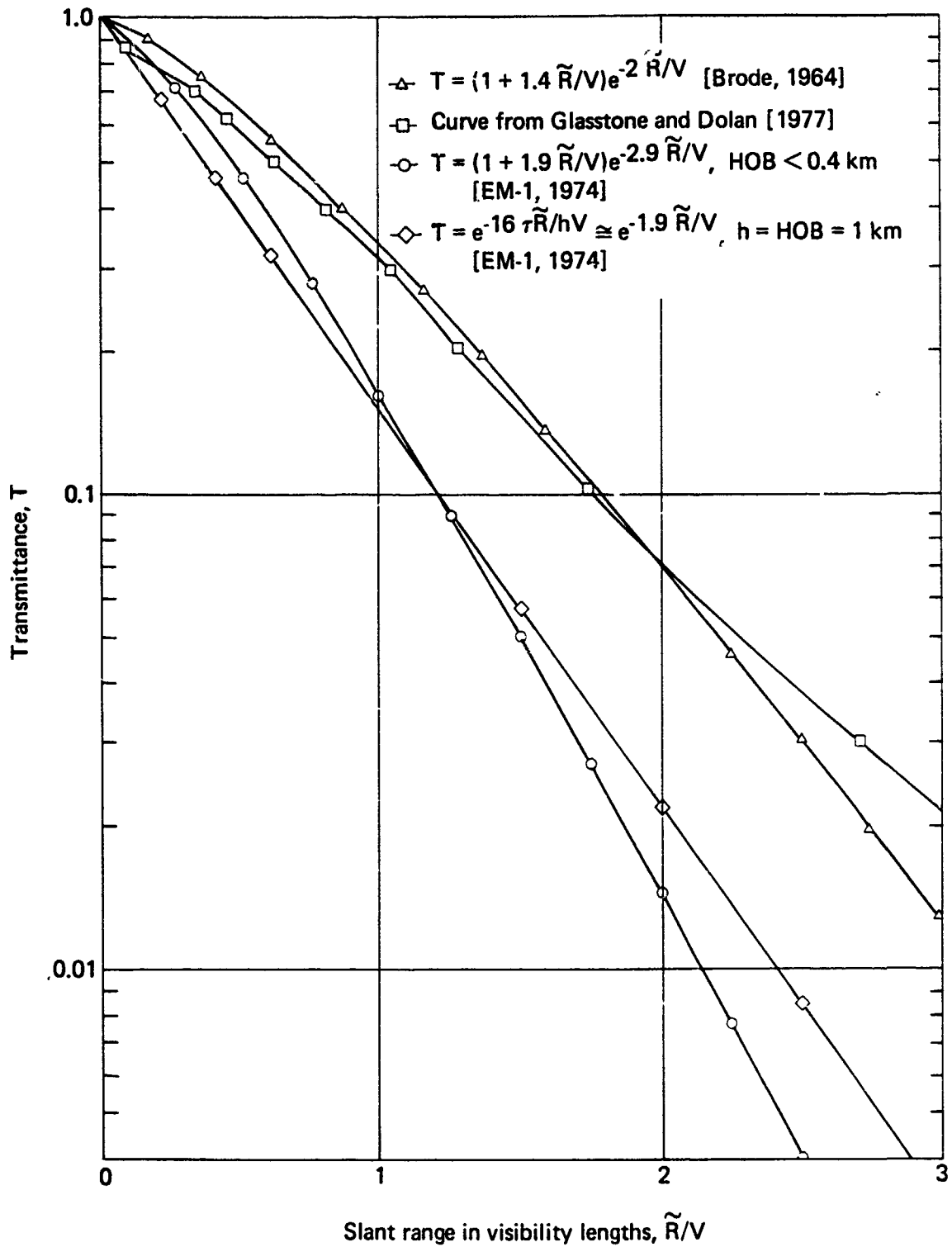


Figure 1. Standard forms for calculating total visible radiation transmissivity from airbursts.

sufficient to adopt a preferred form, so the coefficients α , β as well as the visibility length V were considered as variable parameters and were allowed to assume a range of values.

The target vulnerability to the thermal flux depends on the type and density of the combustible materials and their exposure to the fireball. In general, many modern buildings have large window areas exposing interior fuels susceptible to ignition. Blast disruption of closed structures may also expose combustible materials to the thermal radiation.* Exterior construction materials are also vulnerable, although they are more sensitive to moisture levels and usually require higher flux levels for sustained ignitions to occur.

A typical urban area may have a mixed distribution of residential and commercial/industrial buildings. Each building type will have different contents and hence a different susceptibility. Some industrial facilities may not have many combustible materials and thus a low vulnerability. Others may contain highly volatile materials, and so be vulnerable to even low flux levels. Residential, commercial, and office structures generally contain large amounts of synthetic and cellulosic-type materials, and so have a moderate to high susceptibility to thermal ignitions.

A comprehensive analysis of fire damage from thermally induced ignitions should consider an urban map of structures and the resulting vulnerability distribution. In this initial study, a homogeneous building type and uniform vulnerability is assumed throughout the target area. Specific targets may have smaller or greater vulnerabilities than the median values used in this analysis, but the same procedure could be used to determine the correspondingly increased or decreased damage ranges.

Residential structures contain a wide variety of ignition sources, ranging from newspapers and magazines to wood cabinets and wardrobes. The former materials are easily ignited by low levels of thermal radiation; the latter require substantially greater amounts. Intermediate levels sustain ignitions in drapery, heavy bedding, and padded furniture

*For large weapon yields, a significant fraction of the thermal radiation may be incident after the shock wave arrival [Small and Brode, 1983].

such as sofas or armchairs. The particular ignition threshold depends also on the weapon yield. For a 50 KT explosion, sustained ignition of interior furnishings was assumed 50 percent probable at a flux level of 16 cal/cm^2 . The comparable value for a 1 MT burst was taken to be 22 cal/cm^2 [DNA EM-1(N), 1974; Glasstone and Dolan, 1977].

Greater incident flux levels increase the probability of a fire. We assumed a 90 percent damage probability at 24 cal/cm^2 (50 KT) and 33 cal/cm^2 (1 MT), and similarly 10 percent probability at 8 and 11 cal/cm^2 . At ground zero, the damage probability is 100 percent.

For those three thermal levels Q (for 90, 50, and 10 percent probabilities), the effective damage ranges can be determined from Eq. (1), and a damage distribution created. The influence of variable weapon yield, height of burst, scattering and absorption coefficients, threshold levels, and visibility lengths on the resultant damage-range curve is explored in Figs. 2 through 13.

Figure 2 plots the fire-damage-range curve for a 50 KT burst at $500 \text{ ft/KT}^{1/3}$. * The transmittance relation uses $\alpha = 2.0$, $\beta = 1.4$ [Brode, 1964], and the visibility length varies from 3 to 48 mi. Near most Soviet cities, visibility is expected to extend from 6 to 24 mi at least 90 percent of the time. The possible range shift due to the variable atmospheric conditions is illustrated in Fig. 2. The 50 percent probable damage range is increased by only 5 percent for a visibility length variation of 12 to 48 mi; however, for the bracketed range (3 to 48 mi), there is a 25 percent change.

Figure 3 shows the effect of larger coefficients for extinction ($\alpha = 2.9$) and scattering ($\beta = 1.9$) [DNA EM-1(N), 1974]. The fire damage ranges are all percent less than those in Fig. 2 (50 percent damage level) at the low visibility end (3 mi), but only slightly decreased (1 to 2.5 percent) at the upper range of visibility lengths.

Figures 4 and 5 illustrate the same parameter excursions for a 1 MT burst. Since the increased yield results in a greater thermal reach, the

*In this analysis, most damage-range curves assume a $500 \text{ ft/KT}^{1/3}$ scaled height of burst, since burst height did not appear to be a sensitive variable (see pp. 19 and 22),

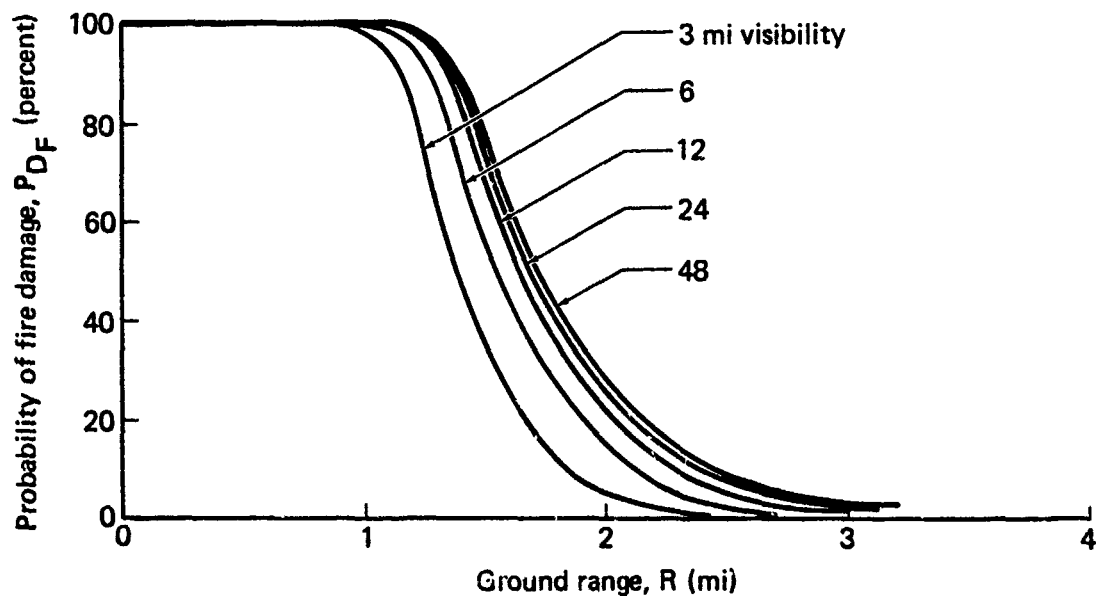


Figure 2. Fire damage range for thermally induced ignitions: variable visibility lengths, $W = 50$ KT, $\alpha = 2.0$, $\beta = 1.4$.

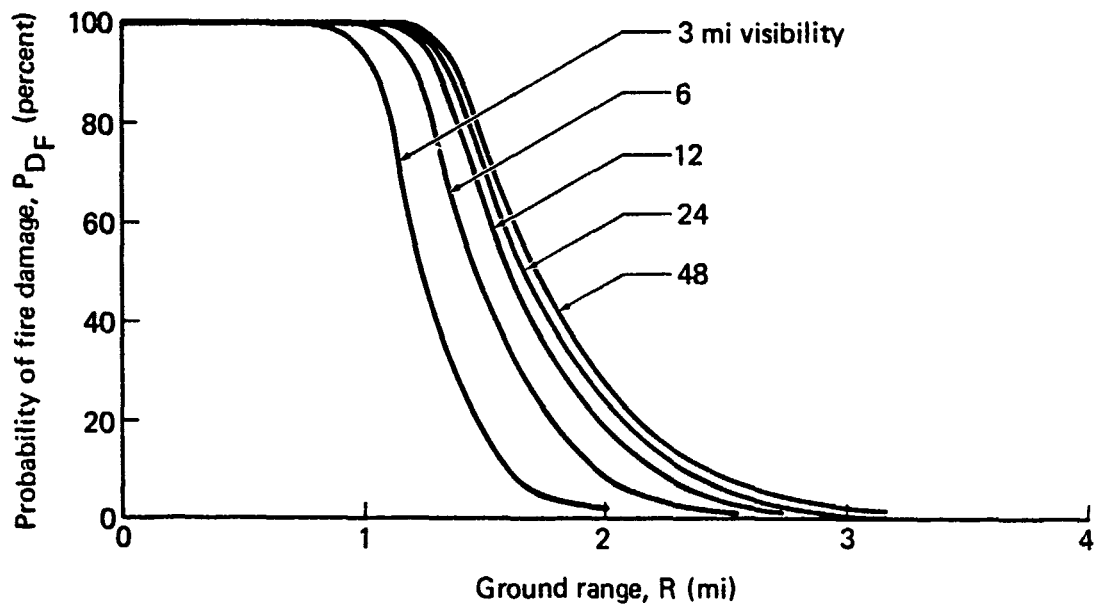


Figure 3. Fire damage range for thermally induced ignitions: variable visibility lengths, $W = 50$ KT, $\alpha = 2.9$, $\beta = 1.9$.

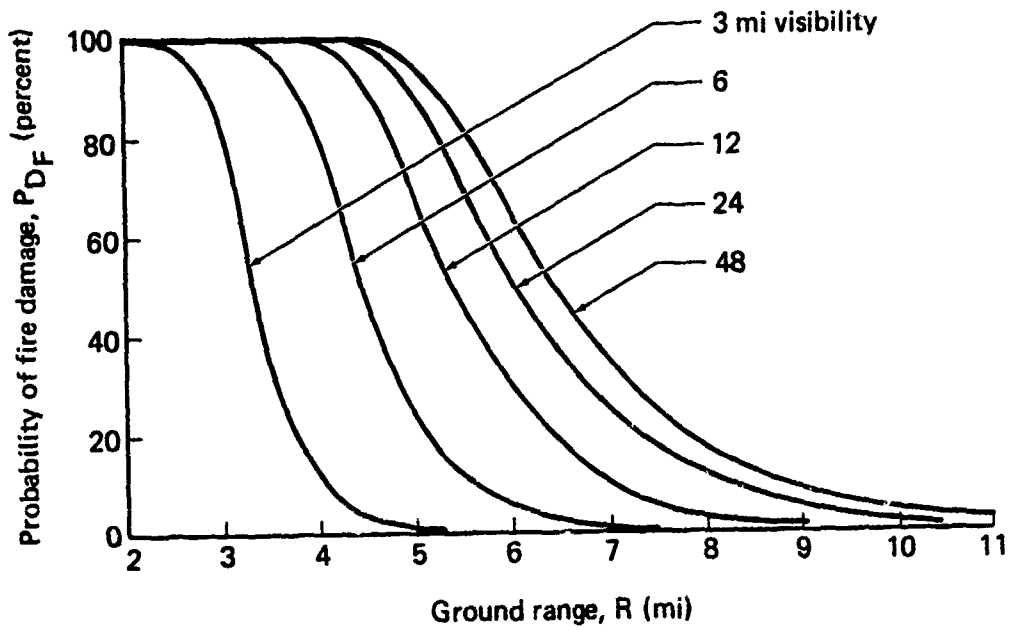


Figure 4. Fire damage range for thermally induced ignitions: variable visibility lengths, $W = 1$ MT, $\alpha = 2.0$, $\beta = 1.4$.

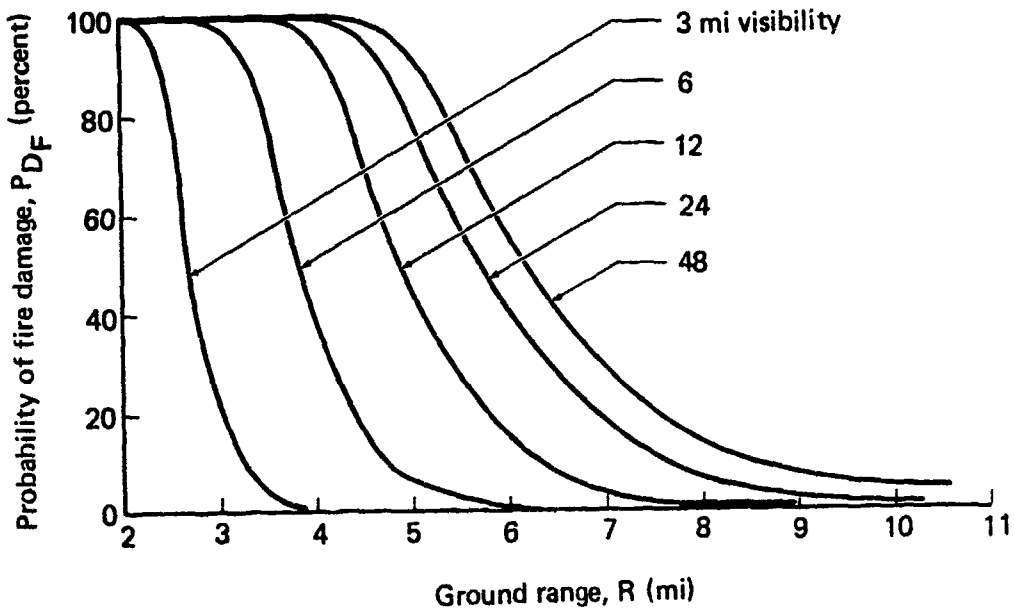


Figure 5. Fire damage range for thermally induced ignitions: variable visibility lengths, $W = 1$ MT, $\alpha = 2.9$, $\beta = 1.9$.

influence of the visibility length is more pronounced. The mean damage range doubles with an increase in the visibility length from 3 to 48 mi (Fig. 4). In the narrower span of 6 to 24 mi, the damage range varies by 33 percent. A somewhat larger variation results from the use of the higher absorption and scattering coefficients (Fig. 5). The higher coefficient values also shorten the effective range for thermally induced ignitions (by about 11 percent at 50 percent P_D for 12 mi visibility).

For thermally induced fires, atmospheric conditions can significantly change the effective fire damage radius. The ranges considered in Figs. 2 through 5 bracket the estimated "extreme" conditions. Statistical analysis of seasonal weather patterns for specific target areas [Fullwood and Tobriner, 1973; Drake, 1982] can reduce the span of likely visibility lengths, thus lessening the variation in the fire damage radius. In particular, large seasonal variations could be removed if the time of year (and time of day) were known. The uncertainty associated with the absorption and scattering coefficients may be reduced through experimental determination of those coefficients for typical urban atmospheres using high-powered light sources.

Because of enhanced scattering, the amount of thermal radiation incident on a target can be modified by either snow or reflecting cloud cover. Simple multiplicative constants (E , A) are used here to describe deviations from the normal ($V = 12$ mi, $\alpha = 2.0$, $\beta = 1.4$) fire-damage-range curve. Factors greater than 1.0 account for thermal radiation enhancement such as may be caused by reflection from superior cloud decks or from snow cover. Figures 6 and 7 display fire-damage-range curves with the radiation enhancement factor E varied from 1.0 to 1.9. For both the 50 KT and 1 MT yields, the damage range can be increased approximately one-third. The effect is slightly greater for lower yields. The high reflection factors for snow and superior clouds significantly extend the damage region.

The influence of radiation attenuation A (from a cloud layer between the burst and the ground) is shown in Figs. 8 and 9. The fourfold reduction in the incident thermal radiation (75 percent of the fireball radiation absorbed by the cloud layer) is assumed representative of heavy

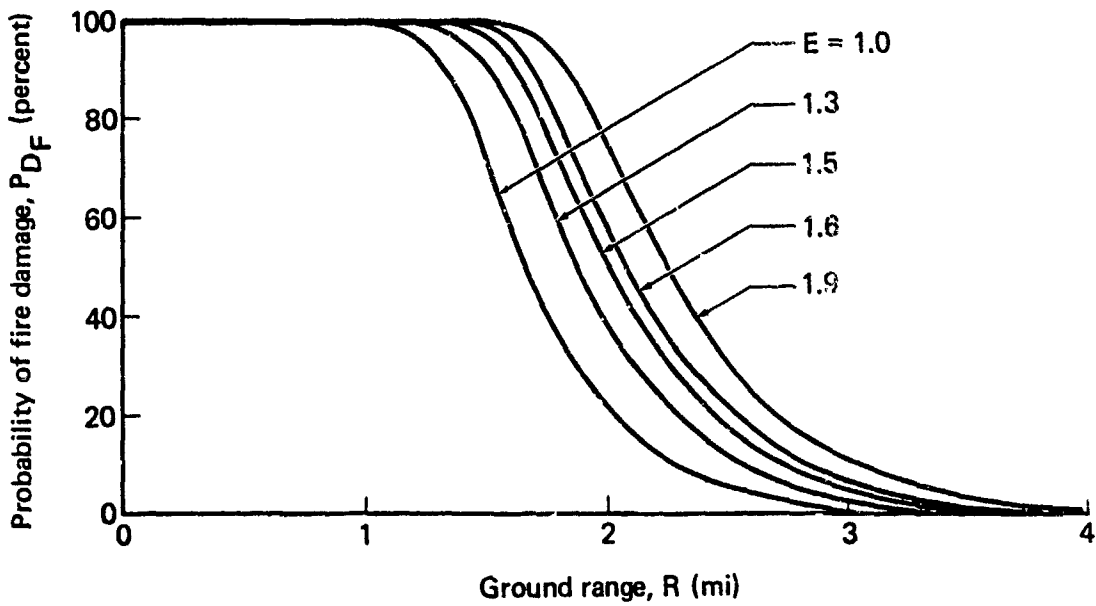


Figure 6. Fire damage range for thermally induced ignitions: variable levels of radiation enhancement, $W = 50$ KT, $V = 12$ mi, $\alpha = 2.0$, $\beta = 1.4$.

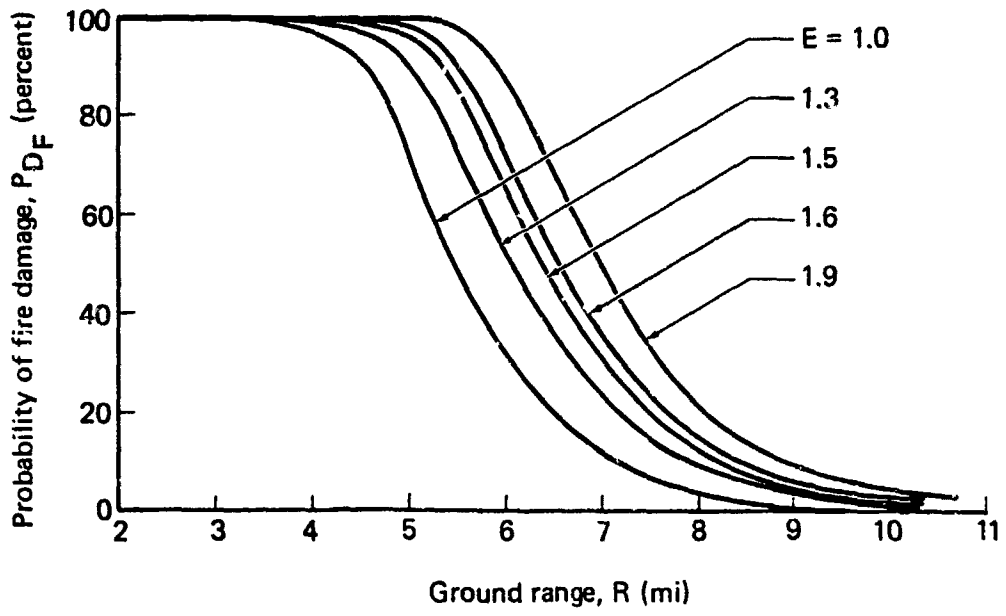


Figure 7. Fire damage range for thermally induced ignitions: variable levels of radiation enhancement, $W = 1$ MT, $V = 12$ mi, $\alpha = 2.0$, $\beta = 1.4$.

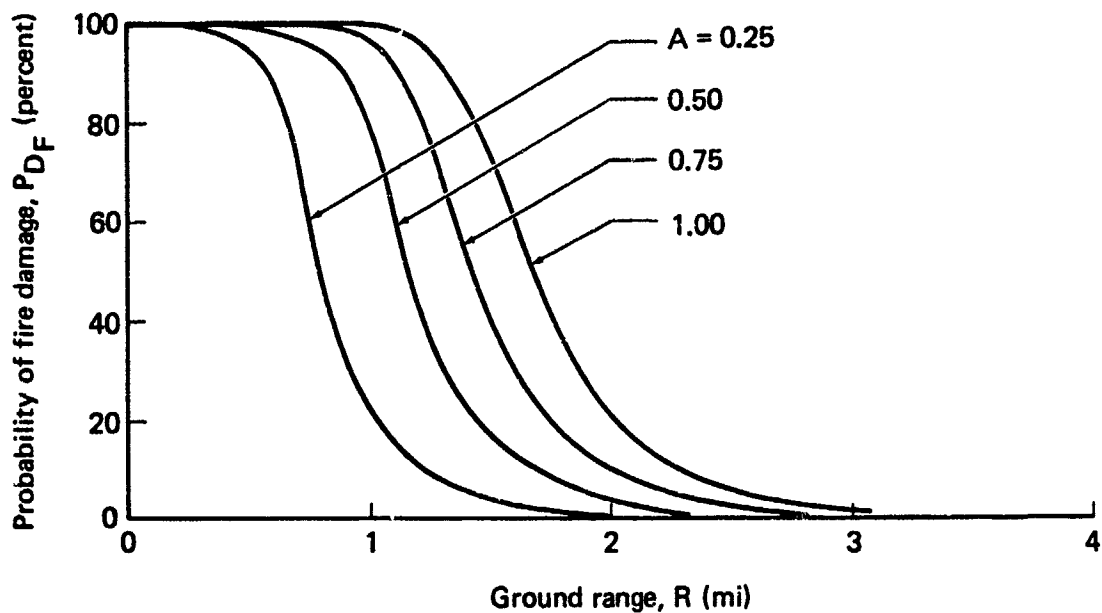


Figure 8. Fire damage range for thermally induced ignitions: variable levels of radiation attenuation, $W = 50$ KT, $V = 12$ mi, $\alpha = 2.0$, $\beta = 1.4$.

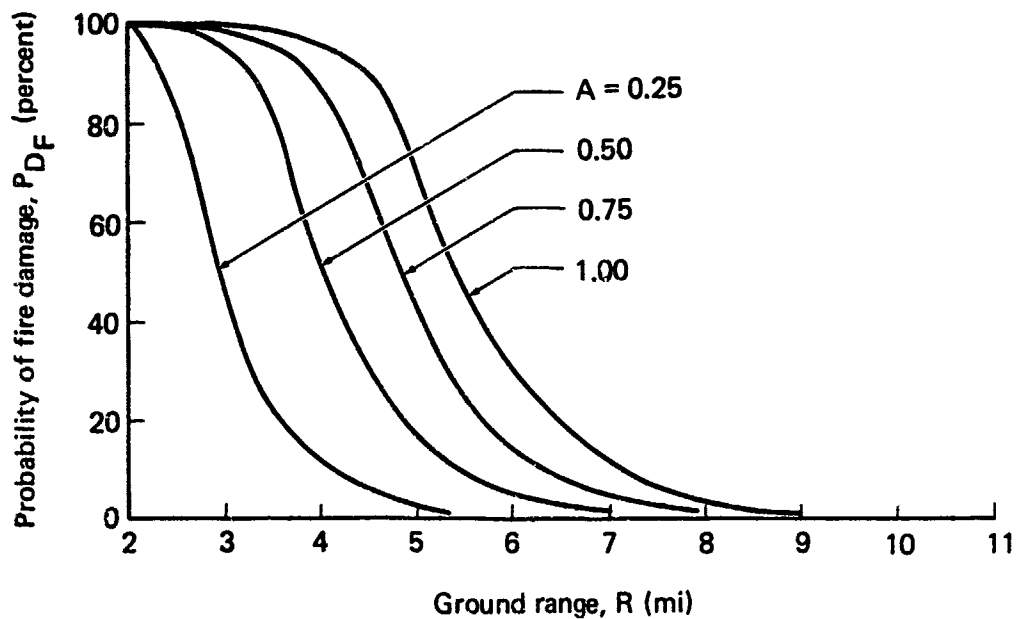


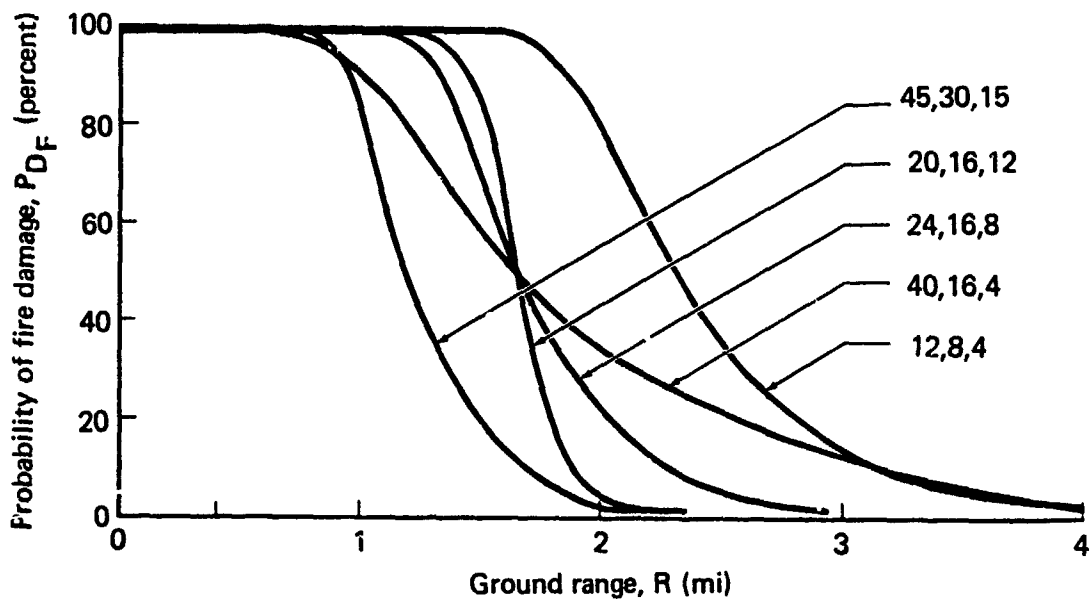
Figure 9. Fire damage range for thermally induced ignitions: variable levels of radiation attenuation, $W = 1$ MT, $V = 12$ mi, $\alpha = 2.0$, $\beta = 1.4$.

cloud cover. For that case, the thermal reach is approximately halved. For both the 50 KT and 1 MT examples, attenuation or cloud absorption of the fireball radiation substantially reduces the damage range for thermally induced ignitions.

The ignition threshold levels used to construct the initial set of damage-range curves were representative of residential structure vulnerabilities, but building usage and the corresponding vulnerabilities may vary widely in a typical urban area. Adjacent buildings may have much different fuel loadings (greater or lesser ignition threshold levels) and hence different damage radii. Without identifying particular industries or building usages, a range of vulnerabilities is now considered and damage-range curves are constructed. As in the previous cases, a homogeneous target area is assumed.

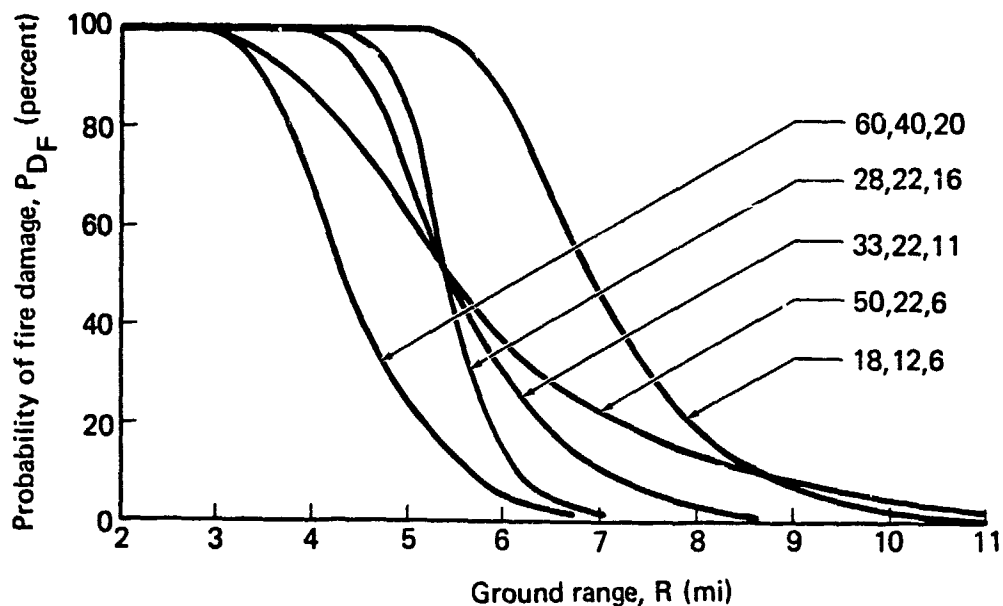
A range of ignition thresholds was assumed for the 10, 50, and 90 percent probabilities of fire damage, and the corresponding radii computed for two yields, 50 KT and 1 MT, and two transmissivity forms. The importance of ignition threshold dependence is illustrated in Figs. 10 through 13. Lower threshold levels significantly extend the damage radius, and higher limits reduce the range. For example, halving (from the nominal values) the threshold limits doubles the probable damage area. The effect is slightly greater for lower yield explosions and for the lesser values of the absorption and scattering coefficients (cf. Figs. 10, 11 and Figs. 12, 13). Adjustment of the 10 and 90 percent vulnerabilities to reflect either greater or lesser variability in the thresholds for fires significantly skews the range curves.

The weapon height of burst also influences the thermal reach and damage radius. For surface bursts, the radiative efficiency of the fireball is reduced considerably by the ingestion of surface materials, and incident thermal fluxes are reduced by dust obscuration. Shading effects are also more significant. As the height of burst increases to an optimum (for radiative effects), the thermal reach increases, but at most operational heights of burst, this range sensitivity to burst height is slight. Some sample heights and effective ranges are shown in Table 1. The effect of variable room exposure due to the changing angle of incidence (7 to 17 deg for 50 KT, 6 to 14 deg for 1 MT) is neglected in those



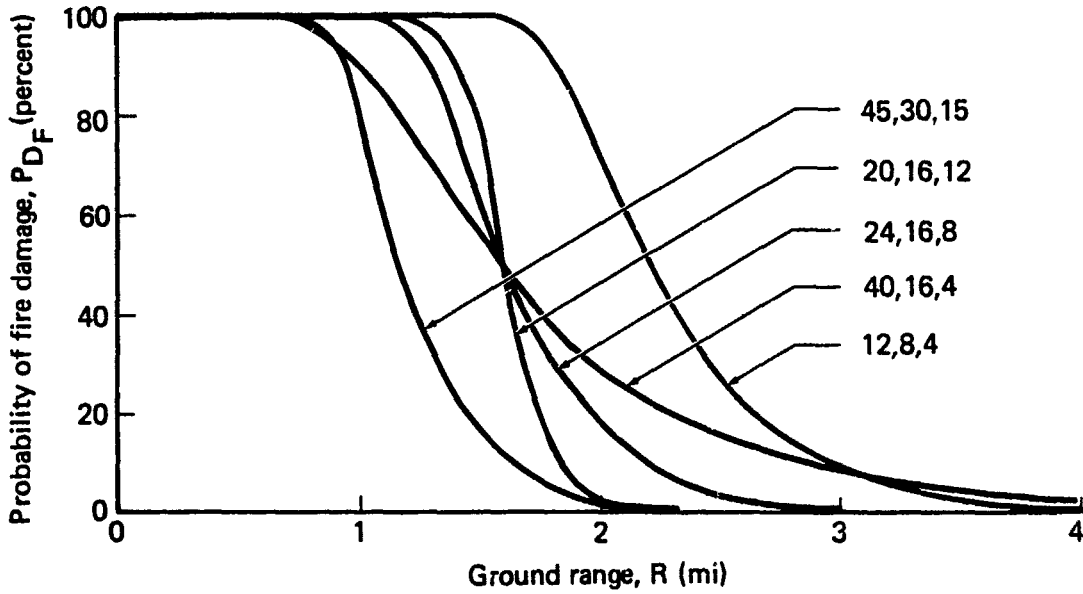
Note: Values identifying each curve represent ignition threshold levels for 90, 50, and 10% fire-start probabilities, respectively.

Figure 10. Fire damage range for thermally induced ignitions: variable ignition threshold levels, $W = 50$ KT, $V = 12$ mi, $\alpha = 2.0$, $\beta = 1.4$.



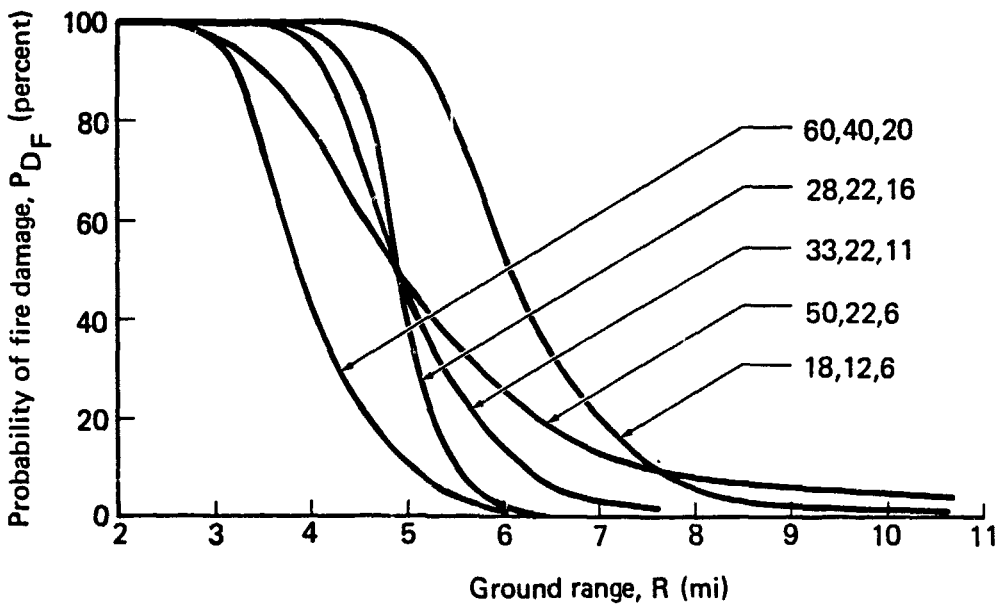
Note: Values identifying each curve represent ignition threshold levels for 90, 50, and 10% fire-start probabilities, respectively.

Figure 11. Fire damage range for thermally induced ignitions: variable ignition threshold levels, $W = 1$ MT, $V = 12$ mi, $\alpha = 2.0$, $\beta = 1.4$.



Note: Values identifying each curve represent ignition threshold levels for 90, 50, and 10% fire-start probabilities, respectively.

Figure 12. Fire damage range for thermally induced ignitions: variable ignition threshold levels, $W = 50$ KT, $V = 12$ mi, $\alpha = 2.9$, $\beta = 1.9$.



Note: Values identifying each curve represent ignition threshold levels for 90, 50, and 10% fire-start probabilities, respectively.

Figure 13. Fire damage range for thermally induced ignitions: variable ignition threshold levels, $W = 1$ MT, $V = 12$ mi, $\alpha = 2.9$, $\beta = 1.9$.

calculations. Mean damage ranges vary by only a few percent for scaled burst heights between 300 and 700 ft/KT^{1/3}. The damage ranges are much more sensitive to yield, threshold levels, visibility, and radiation enhancement or attenuation factors than to burst height.

Table 1. Effect of burst height on fire damage range.

Scaled Burst Height (ft/KT ^{1/3})	Actual Burst Height (ft)	Scaled Ground Range (ft/Y.T ^{1/3})	Peak Overpressure (psi)
<i>50 KT Yield, 16 cal/cm² Ignition Threshold</i>			
700	2580	2305	4.2
500	1840	2355	3.4
300	1105	2390	3.0
<i>1 MT Yield, 22 cal/cm² Ignition Threshold</i>			
700	7000	2800	3.0
500	5000	2845	2.6
300	3000	2870	2.2

NOTE: V = 12 mi, α = 2.0, β = 1.4.

SECTION 4

BLAST-INDUCED IGNITIONS

Fires are also likely to result from blast-induced disruptions. Ignitions may develop from the spilling of volatile liquids located in industrial, commercial, and residential structures or vehicles, or from the disruption of hot or molten materials, sparks near volatile or explosive fuels, gas line ruptures, short circuits, reacting chemical mixtures, etc. The blast wave is the disruptive agent, although ground shock and synergistic effects with the late thermal radiation may also contribute to the ignitions.

The particular interaction that ends in a fire start may be very obscure. The structure hardness (possibly identified by a VN designation), type and location of sources, overpressure, electrostatic discharge, flying debris, and late thermal radiation all are important variables that may determine the probability of a blast-induced fire start. Data that could support correlations are scarce (see, for example, McAuliffe and Moll [1965]), and analytical prediction procedures have not yet been developed. Intuition suggests that the probability of a fire start should depend primarily on the blast wave strength and on the target blast resistance. The former is easily mapped [Speicher and Brode, 1980, 1981; Brode, 1983]. The latter requires some target knowledge, model development, and experimental verification.

Based on the presumed occurrence of blast-induced ignitions at Hiroshima and Nagasaki, McAuliffe and Moll [1965] proposed a "secondary" fire frequency of 0.006 per 1000 ft² of building floor area damaged. Although the fire start distribution is not a function of overpressure (or dynamic pressure), the dependence is implicit. Owing to the paucity of data, a more detailed prediction scheme was not considered warranted.

Wilton, Myronuk, and Zaccor [1981] developed a secondary fire-start model that classifies the hardness of a facility and its contents and relates the resultant fire vulnerability to the shock wave overpressure. Since there are no new experimental or survey data, the model assumptions

remain unjustified. However, the method does provide an estimate of blast-induced fire starts consistent with general intuition. Further work could refine the model and reduce the uncertainties. For this study, the method of Wilton, Myronuk, and Zaccor [1981] was used to estimate blast-induced fire start distributions.

The radius of a probable fire start increases as the structure blast resistance is reduced, the number of potential sources increased, or the ignition susceptibility increased. Several examples are shown in Table 2 and Figs. 14 and 15. As in Sec. 3, a homogeneous target area is assumed. In general, probable damage ranges for different city areas or even adjacent buildings may vary widely.

The probability distribution defined in Table 2 is discontinuous at several overpressures as the damage classification changes from heavy to medium to light. The distribution depends critically on the designation of building type and contents.* The discontinuities in probability are somewhat smoothed in the fire-damage-range curves shown in Figs. 14 and 15.

As the vulnerability increases, large changes result in the probable damage radius. Light-design structures (type 10) with highly flammable contents (approaching 10) present a high probability of blast-induced fires out to and beyond 0.5 psi regions (5 to 9 mi for a 50 KT burst, 13 to 24 mi for a 1 MT burst). Damage ranges estimated for even the medium-design-load structures with moderate contents indices are comparable to or greater than ranges for thermally induced ignitions.

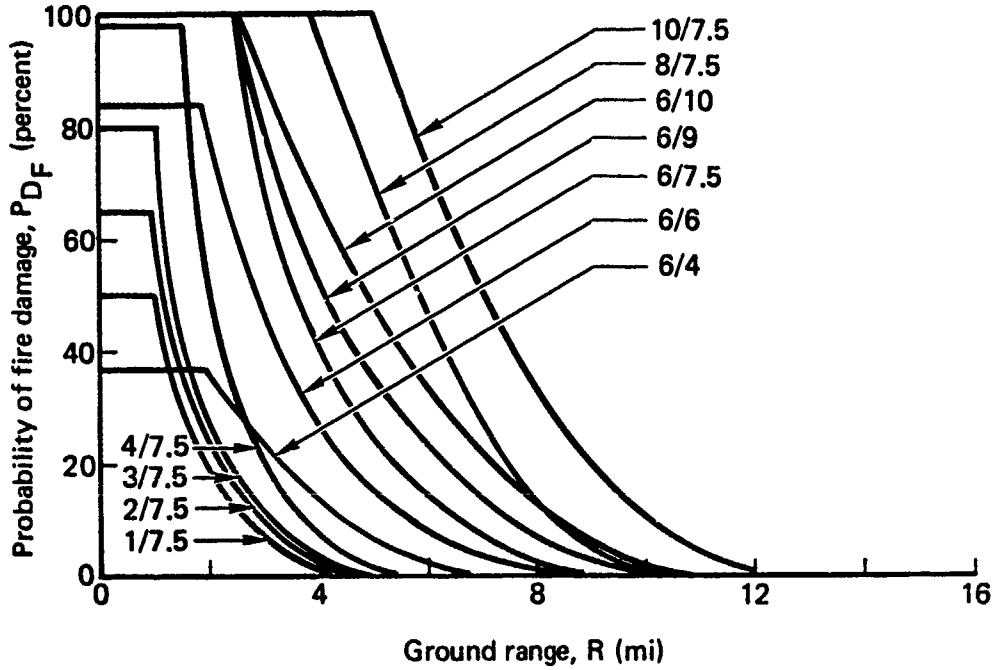
* Wilton, Myronuk, and Zaccor [1981, Tables 16 and 17, pp. 61-63]. Both indices range from 1 to 10. Building type 1 represents a heavy design load (reinforced concrete structures designed for protection, such as bank vaults); and type 10, a light design load (structures with wood/metal stud walls and siding or light corrugated metal walls and roofs, such as residences or storage sheds). Contents type 1 represents materials of low flammability; and type 10, highly flammable, explosive materials.

Table 2. Probabilities of blast-induced ignition.

Peak Overpressure (psi)	Ground Range (mi)		Blast Damage Level			Ignition Probability (percent)	
	50 KT ^a	1 MT ^a	Building Type 4	Building Type 5	Building Type 4, Contents Type 7.5	Building Type 5, Contents Type 8.5	
7	1.1	2.8	Heavy	Heavy	100	100	100
6	1.2	3.2	Heavy	Heavy	100	100	100
5	1.3	3.6	Heavy	Heavy	100	100	100
4	1.5	4.2	Heavy	Heavy	100	100	100
3	1.9	5.0	Heavy/ medium	Heavy/ medium	100/8	100/8	100/8
2	2.5	6.6	Medium	Medium	8	8	8
1	4.0	11.0	Medium/ light	Medium	8/3	2	2
0.75	4.7	13.0	Light	Medium/ light	3	2/1	2/1
0.50	6.4	17.0	Light	Light	3	1	1

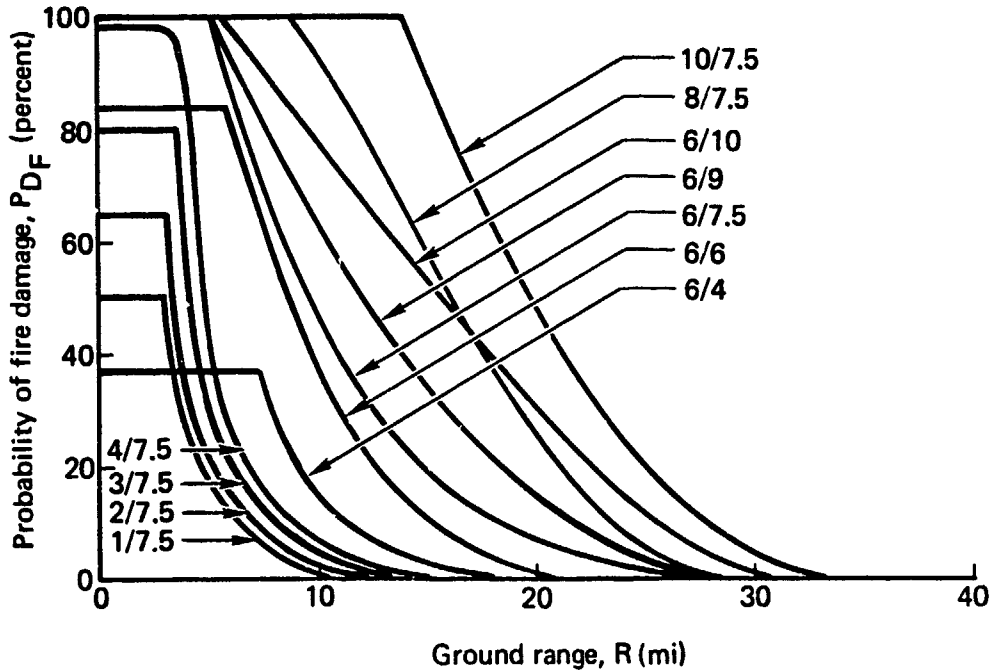
NOTE: These probabilities were calculated using the empirical method and indices of building types and contents specified by Wilton, Myronuk, and Zaccor [1981, Tables 16 and 17, pp. 61-63].

^aAt a 500 ft/KT^{1/3} scaled height of burst.



Note: a/b refers to building type and building contents indices.

Figure 14. Fire damage range for blast-induced ignitions: variable building type/contents indices, $W = 50$ KT.



Note: a/b refers to building type and building contents indices.

Figure 15. Fire damage range for blast-induced ignitions: variable building type/contents indices, $W = 1$ MT.

SECTION 5

INITIAL FIRE STARTS--COMBINED IGNITION DISTRIBUTION

The distribution of fire damage from the direct weapon effect-target interaction is derived by summing the probabilities of thermally and blast-induced ignitions ($PDF = P1 + P2 - P1 \times P2$). Damage-range curves representing the combined effects are shown in Figs. 16 and 17. The blast-induced ignitions are based on fixed building type/contents indices of 4/7.5. Those values are assumed typical of the bulk of urban area buildings.

Mean damage ranges for the combined effects are significantly greater than either of the component ranges. In addition, the region of total or uniform destruction ($PDF = 100$ percent) is much larger. Only moderate sensitivity to attenuation of the thermal radiation (cf. Figs. 6 through 9) occurs, since inclusion of blast-induced ignitions lessens the influence of those parameters (i.e., short visibility lengths or high levels of absorption by cloud decks). Similarly, only moderate changes result from variation of the atmospheric transmissivity form. Those parameters would be more important, however, if the distribution of blast-induced ignitions had been greatly exaggerated.

Combining the probabilities of thermally and blast-induced ignitions may compensate for (or mask) inaccuracies in either distribution. Verification of both damage-range relations is needed. A more specific analysis of the sources of blast-induced fires in cities would be valuable. Such sources may be electrical, thermal, chemical, mechanical, electrostatic, or gas dynamic. Certain industries, such as explosives facilities, chemical plants, oil refineries, or power generators, contain obvious potential secondary sources, and could be targeted accordingly. Such features, when identifiable, should be part of the vulnerability number designation since the ensuing fires are likely to extensively damage some facilities that might otherwise survive the blast. Such was the case for an electrical generating station in Hiroshima--though housed in a massive building that survived the blast, the station itself was gutted by fire.

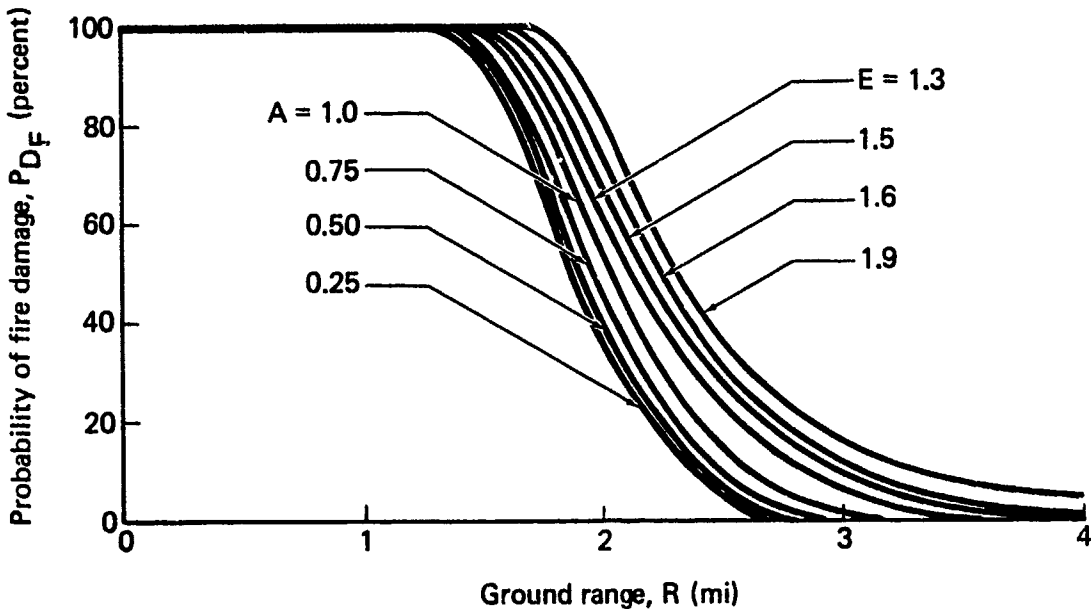


Figure 16. Fire damage range for thermally and blast-induced ignitions: variable levels of radiation attenuation and enhancement, $W = 50$ KT, $V = 12$ mi, $\alpha = 2.0$, $\beta = 1.4$, building type/contents index = 4/7.5.

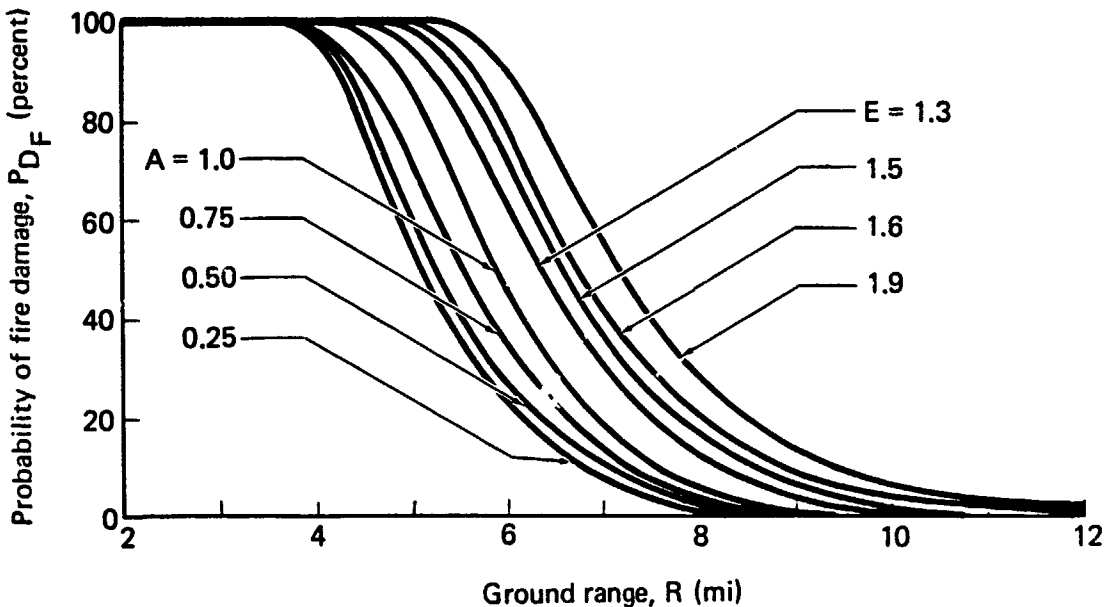


Figure 17. Fire damage range for thermally and blast-induced ignitions: variable levels of radiation attenuation and enhancement, $W = 1$ MT, $V = 12$ mi, $\alpha = 2.0$, $\beta = 1.4$, building type/contents index = 4/7.5.

SECTION 6

FIRE SPREAD

The spot ignitions developing from the immediate thermal or shock wave-target interactions are likely to lead to full structure fires in approximately 15 to 30 min, but less if immediate flashover occurs.* The many thousands of early fires grow and spread and are often sufficient to generate high-velocity winds, generally flowing toward the inner portions of the burning region. Mean velocities of order 20 to 40 m/sec may be typical [Larson and Small, 1982a,b]. Such high-velocity fire winds indicate a high probability of spread between buildings. Possible spread mechanisms include wind-aided flame spread, fire brand transport, and radiative heating from inclined flame fronts.

In general, random spot fires in wildland and urban fire areas tend to spread rapidly, greatly multiplying the total damage (see, for example, Pyne [1982]). A city subject to a nuclear weapon explosion is likely to have extensively damaged regions with widely scattered debris and many thousands of fires. For such conditions, fire spread throughout much of the target area is probable. The extensive blast damage, debris buildup, radioactive fallout, and threat of subsequent bursts are likely to deter or render ineffective most trans- or postattack firefighting.

Many of the variables that influence fire spread in a damaged city may be identified. However, synthesis of all these factors into one theory remains a formidable task [Sanderlin, Ball, and Johanson, 1981]. Without explicitly treating the physical mechanisms of spread a heuristic accounting for the long-time spread damage is used to modify the damage-range relation. The initial estimate assumes that the probability of fire damage at any radius is doubled when spread is included. Thus, if 50 percent of the structures are burning, it is assumed that the fire will spread to all adjacent structures. Similarly, ignition in one building

* An immediate flashover was observed in a room exposure in the atmospheric nuclear test ENCORE of the UPSHOT-KNOTHOLE series (26 KT at a scaled burst height of nearly $800 \text{ ft/KT}^{1/3}$).

in four implies fire damage to half of the structures. The estimation, though crude, is hopefully conservative (i.e., does not overestimate the increase in damage due to spread).

Damage-range curves showing the combined effects of initial ignitions and later spread are shown in Figs. 18 and 19. The uncertainty inherent in the initial (thermal) ignition distribution is still indicated by the bracketing curves for enhanced or attenuated thermal flux levels. The inclusion of spread using the assumed model (doubling of damage probabilities) not only increases the region of complete damage, but leads to a rapid drop to low probabilities of damage. This result is consistent with the near-complete damage and fairly well-defined fire perimeter observed at Hiroshima [Bond, 1951].

The damage ranges shown in Figs. 18 and 19 are based on spread of the initial thermally and blast-induced ignitions. A less conservative valuation of the vulnerability to blast-induced ignitions (higher building or contents indices) or even a mixed distribution of vulnerabilities may significantly enlarge the damage radii. For the cases considered, complete fire damage extended beyond the 3 psi region (1.9 mi for 50 KT, 5 mi for 1 MT), even for the greatest assumed values of radiation attenuation ($A = 0.25$).

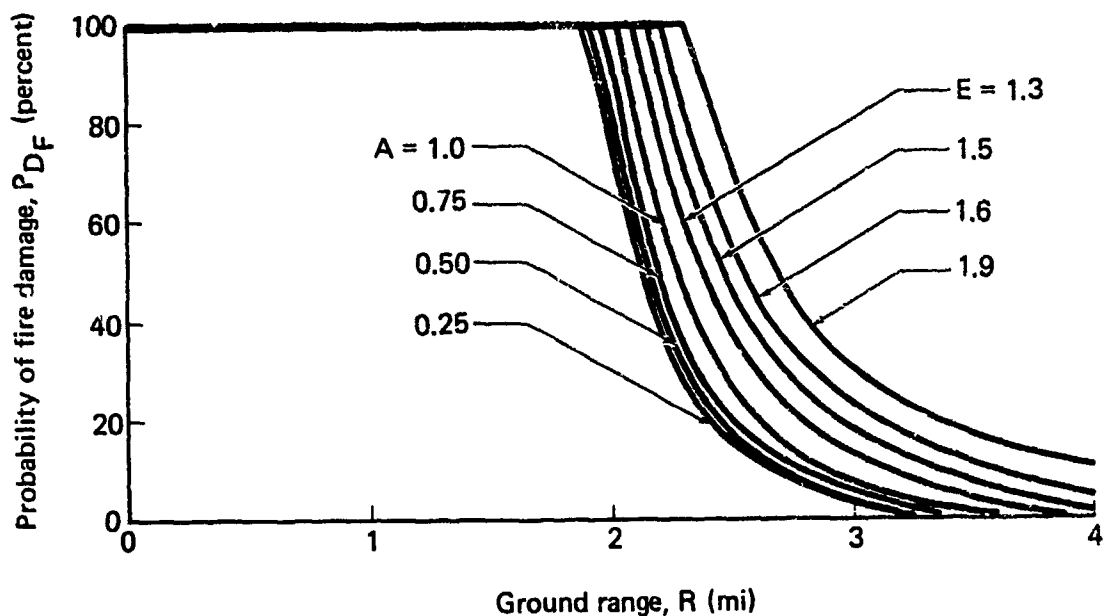


Figure 18. Fire damage range for thermally and blast-induced ignitions and fire spread: variable levels of radiation attenuation and enhancement, $W = 50 \text{ KT}$, $V = 12 \text{ mi}$, $\alpha = 2.0$, $\beta = 1.4$, building type/contents index = $4/7.5$.

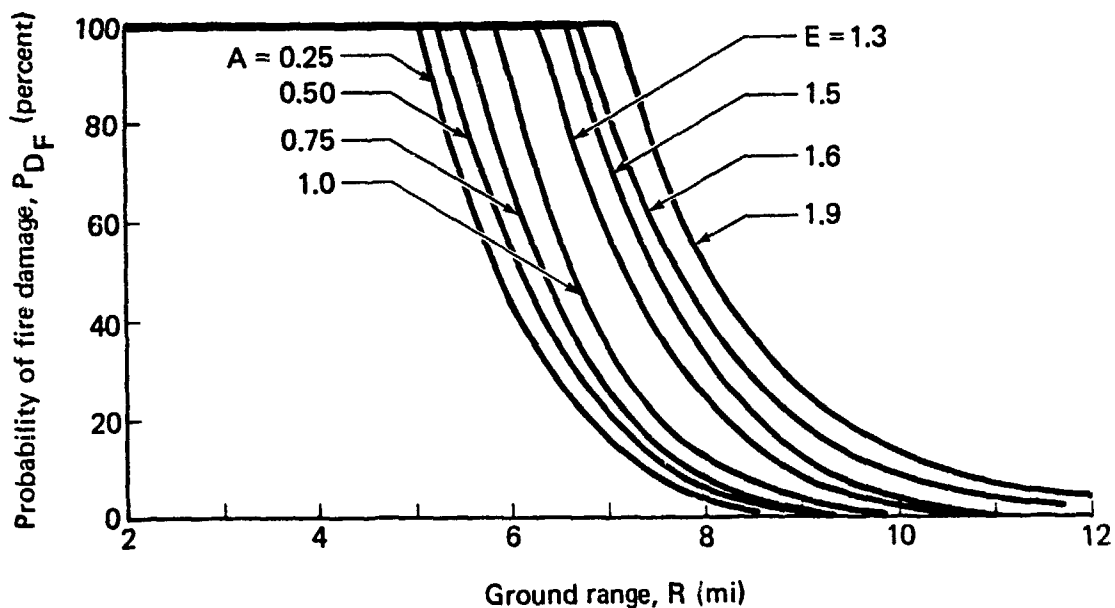


Figure 19. Fire damage range for thermally and blast-induced ignitions and fire spread: variable levels of radiation attenuation and enhancement, $W = 1 \text{ MT}$, $V = 12 \text{ mi}$, $\alpha = 2.0$, $\beta = 1.4$, building type/contents index = $4/7.5$.

SECTION 7
CIVIL DEFENSE

The inadequacy of active and organized fire suppression in Japan may have contributed to much higher levels of destruction and casualties in the fire bombing during the last six months of World War II. Conversely, over four years of increasingly intense air war, well-organized and well-equipped German civil defense crews developed mitigation and rescue techniques that were successful in minimizing the loss of lives and restricting the property damage.

Similar efforts, however, may not be as effective prior to or following a nuclear weapon burst. Widespread blast effects would incapacitate local firefighters and equipment, unless they were sheltered or evacuated during the attack. In addition, debris buildup may limit mobility, while subsequent bursts could further impede a vigorous or prompt response by even a well-organized civil defense. Even with reliable warning, firefighters may choose to remain sheltered. The possibility of radioactive fallout or rainout presents an additional hazard and, thus, a further deterrent to firefighting activities. Nevertheless, effective firefighting and rescue measures potentially could limit damage and loss of life during large urban fires, even those ignited by nuclear bursts.

Figures 20 and 21 compare the effectiveness of civil defense preparations against various types of ignitions and fire spread for a 50 KT and a 1 MT burst. Preattack protective measures were assumed to reduce the probabilities of thermally and blast-induced ignitions by 50 percent at all ranges. (The probability of thermally induced ignitions still approaches 100 percent since, close to ground zero, the blast wave will disturb the target prior to thermal loading.) The solid curves show the ameliorating effects of civil defense (e.g., reflective window coverings, shut-down of central gas and electric lines) in reducing thermally and blast-induced ignitions and fire spread. For comparison, the dashed fire-damage-range curve duplicates the results for no enhancement or attenuation of thermal radiation ($E, A = 1.0$) shown in Figs. 18 and 19.

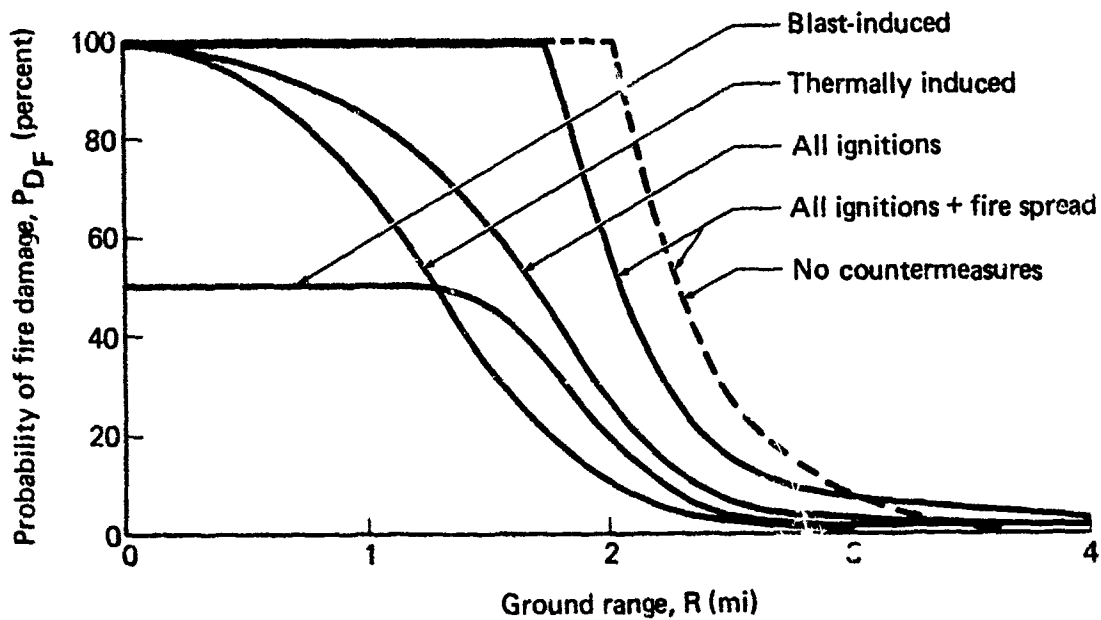


Figure 20. Fire damage range for various combinations of fire starts and spread with and without countermeasures: $W = 50 \text{ KT}$, $V = 12 \text{ mi}$, $\alpha = 2.0$, $\beta = 1.4$, building type/contents index = 4/7.5.

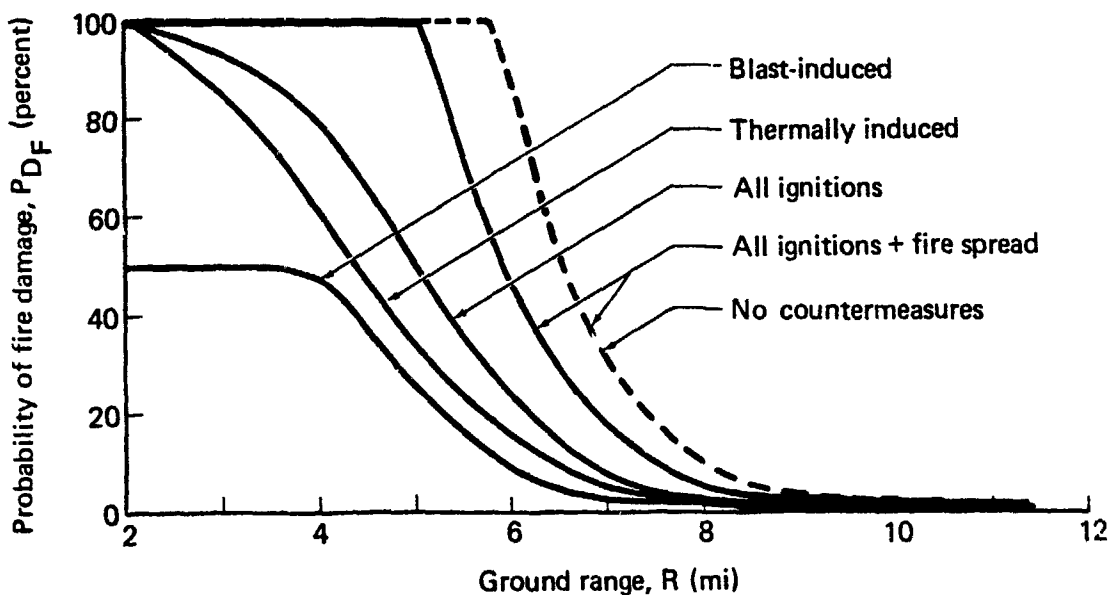


Figure 21. Fire damage range for various combinations of fire starts and spread with and without countermeasures: $W = 1 \text{ MT}$, $V = 12 \text{ mi}$, $\alpha = 2.0$, $\beta = 1.4$, building type/contents index = 4/7.5.

Despite the 50 percent reduction in the distribution of initial ignitions, the mean damage range is reduced by just 10 percent. Increased fire-fighting efforts after the burst could lessen the probability of fire spread, further reducing the effective damage range.

SECTION 8

COMBINED-PARAMETER VARIATIONS

Fires in an attacked urban area result from thermally and blast-induced ignitions or from the subsequent spread to other structures. Many factors modify the ultimate fire distribution. In Secs. 3 through 6, the direct weapon effect-target interactions were estimated, and the effects of modifying influences such as visibility length, transmittance, weather, and variable target vulnerability were considered. The initial ignition curves were modified to include fire spread in Sec. 6, and an accounting for countermeasures was made in Sec. 7. The sample results indicate the basic trends. However, they do not fully include the integrated effects of all the modifying variables. Combining all the effects into a set of mean and standard deviation damage-range curves provides a fairer measure of the uncertainties associated with a spectrum of possible target conditions and vulnerabilities. Such fire-damage-range relations are developed in this section.

Nine specific factors were considered and each assumed to be an "independent" variable. They include ignition threshold level, visibility length, transmissivity form, thermal radiation enhancement due to reflecting clouds or snow, attenuation of thermal radiation by intervening cloud cover, building type/contents indices for blast-induced fires, probability of fire spread, and the effectiveness of countermeasures against both thermally and blast-induced ignitions. Based on the previous excursions, an ensemble of variables was arranged. One- and two-standard-deviation bracketing values were then estimated. Interpolation between the mean and $\pm 1\sigma$ deviation values gave $\pm 1/3\sigma$ and $\pm 2/3\sigma$ values for each variable. These nine factors were assumed to be independent, and on that basis were summed to form $\pm 1\sigma$ and $\pm 2\sigma$ fire-damage-range curves for the combined effects.

Table 3 lists the parameter values chosen for each variable. The spread of values anticipates a wide variety of target conditions and vulnerabilities. Two weapon yields (50 KT and 1 MT) are considered,

Table 3. Ensembles of parameter values.

Parameter	Parameter Value								
	-2σ	-σ	-2/3σ	-1/3σ	Mean	+1/3σ	+2/3σ	+σ	+2σ
50 KT^a ignition threshold (cal/cm²)									
90% probability	51	38	33	29	24	21	18	15	8
50% probability	34	25	22	19	16	14	12	10	5
10% probability	17	13	11	10	8	7	6	5	3
1 MT^a ignition threshold (cal/cm²)									
90% probability	60	47	42	37	33	30	27	25	18
50% probability	40	31	28	25	22	20	18	17	12
10% probability	20	16	14	12	11	10	9	9	6
Visibility length (km)	2	5	7	9	11	22	35	46	92
Transmissivity^b									
α	3.2	2.9	2.75	2.60	2.45	2.30	2.15	2.0	1.8
β	2.0	1.9	1.82	1.73	1.65	1.56	1.48	1.4	1.25
Thermal radiation enhancement (%)									
Snow	--	--	--	--	10	30	50	70	90
Clouds above	--	--	10	20	27	31	35	40	50
Thermal radiation reduction (%)									
Clouds below	85	75	52	28	5	2	--	--	--
Combined effects ^c	0.15	0.25	0.53	0.86	1.33	1.67	2.03	2.4	2.9
Building type/contents indices for blast-induced fires									
	3/2.5	4/4	4.66/4.33	5.33/4.66	6/5	6.33/5.33	6.66/5.33	7/6	9/7.5
Probable fire-spread enhancement factor									
	1.1	1.25	1.5	1.75	2.0	2.3	2.7	3.0	5.0
Reduction of ignitions due to countermeasures (%)									
Thermally induced fires									
Overpressure ≤ 0.5 psi	75	63	58	54	50	43	37	30	10
Overpressure = 2 psi	50	33	31	28	25	22	18	15	5
Overpressure ≥ 5 psi	20	10	7	3	--	--	--	--	--
Blast-induced fires									
Overpressure ≤ 2 psi	80	60	53	47	40	35	30	25	10
Overpressure ≥ 5 psi	80	50	40	30	20	17	13	10	--

^aHeight of burst = 500 ft/KT^{1/3}.

^b[1 + β(R/V)] exp [-α(R/V)].

^cThe multiplication factor is calculated as follows: threshold/combined effect = adjusted incident radiation.

and, for each case, ignition threshold levels were defined for 10, 50, and 90 percent probabilities of a fire start. Worst-case scenarios are represented by the negative standard deviation values. Lower threshold levels corresponding to greater slant ranges are associated with positive standard deviation sets.

The mean visibility length (11 km) represents an average urban clear day. Positive and negative unit standard deviations span the range of conditions from foggy to very clear days. In view of the uncertainty in the relations describing the transmittance of thermal radiation, mean absorption (α) and scattering (β) coefficients were calculated from the average of the values given by DNA EM-1(N) [1974] and Brode [1964]. The lower estimates of α and β correspond to an increase in damage range and thus were used for the positive standard deviation ensembles. Values corresponding to the DNA EM-1(N) [1974] fit were used for the -1σ ensembles. Intermediate values were obtained by interpolating between the mean and $\pm 1\sigma$ sets.

For each ensemble, a probable degree of incident thermal radiation enhancement or attenuation was hypothesized. The mean case postulates a modest probability of thermal radiation enhancement by reflection, and a slight probability of attenuation due to cloud scatter and absorption. The worst-case scenarios admit attenuation only, and the standard deviation sets ($\geq 2/3\sigma$) admit enhancement only. The adjusted incident radiation level necessary to produce a thermally induced ignition was determined for each ensemble by dividing the threshold radiation by the following modification factor (representing the combined effects of reflection and attenuation):

$$CRA = (1 + E_1)(1 + E_2)(1 - A) , \quad (2)$$

where E_1 and E_2 represent the fractional enhancement by radiation reflection from snow cover (E_1) and a superior cloud deck (E_2). The quantity $(1 - A)$ defines the fractional reduction of incident thermal radiation by cloud cover beneath the burst.

Variable building type and contents indices (cf. Figs. 14 and 15) are used to account for differing target susceptibilities to blast-induced

ignitions. The building type index was varied from 3 (worst cast, corresponding to heavy-design-load structures) to a $+2\sigma$ value of 9 (light wood-frame construction). Similarly, the contents type index assumes values from 2.5 (-2σ ensemble) to 7.5. Average parameter values of building type 6 and contents type 5 were used for the mean set.

A constant multiplication factor applied at each point in the damage probability distribution was used to determine the increased probability of damage by fire spread. Fire spread increased the probability of damage by 10 percent for the -2σ set, and by 500 percent for the $+2\sigma$ set. The number of structure fires was doubled for the mean case.

The final two independent variables used in each ensemble accounted for the reduction in ignitions due to countermeasures. Countermeasures that reduce the vulnerability to thermally induced ignitions (e.g., reflective window coverings) are distinguished from those that reduce the vulnerability to blast-induced ignitions (e.g., shut-down of central power and gas supplies). In both cases, the effectiveness of the countermeasures is assumed to be a function of the overpressure. The reduction in the number of fire starts is greatest at the lower overpressure levels. The ameliorating effects are assumed to be more pronounced for the blast-induced ignitions. The overall effectiveness decreases for the positive standard deviations.

The mean, $\pm 1/3\sigma$, and $\pm 2/3\sigma$ probability curves for thermally induced ignitions are plotted in Figs. 22 and 23. All modifications to the distribution of primary ignitions (cloud cover, visibility length, transmissivity, countermeasures, and reflectance from snow cover) are included in the dashed curves. The solid curves illustrate the variation excluding the effect of countermeasures. Since the civil defense preparations are assumed most effective at the lower overpressures (≈ 0.5 psi), the fire-damage-range variation is not significantly changed.

The effect of countermeasures is more pronounced in the distribution of blast-induced fires. The solid curves (Figs. 24 and 25) illustrate the fire damage range without countermeasures and the dashed curves trace the variation with countermeasures included.

Fire-damage-range curves representing the sum of the nine independent factors are shown in Figs. 26 (50 KT) and 27 (1 MT). The mean curves are

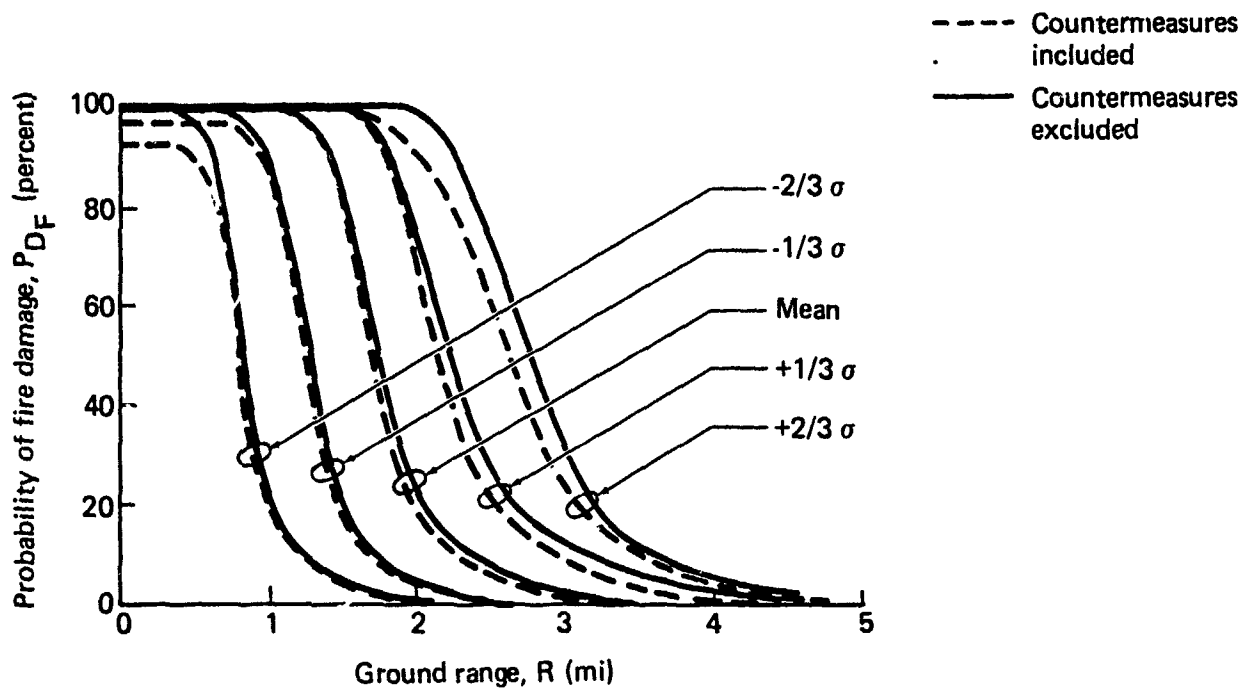


Figure 22. Fire damage range for thermally induced ignitions: combined-parameter variations with and without countermeasures, $W = 50$ KT.

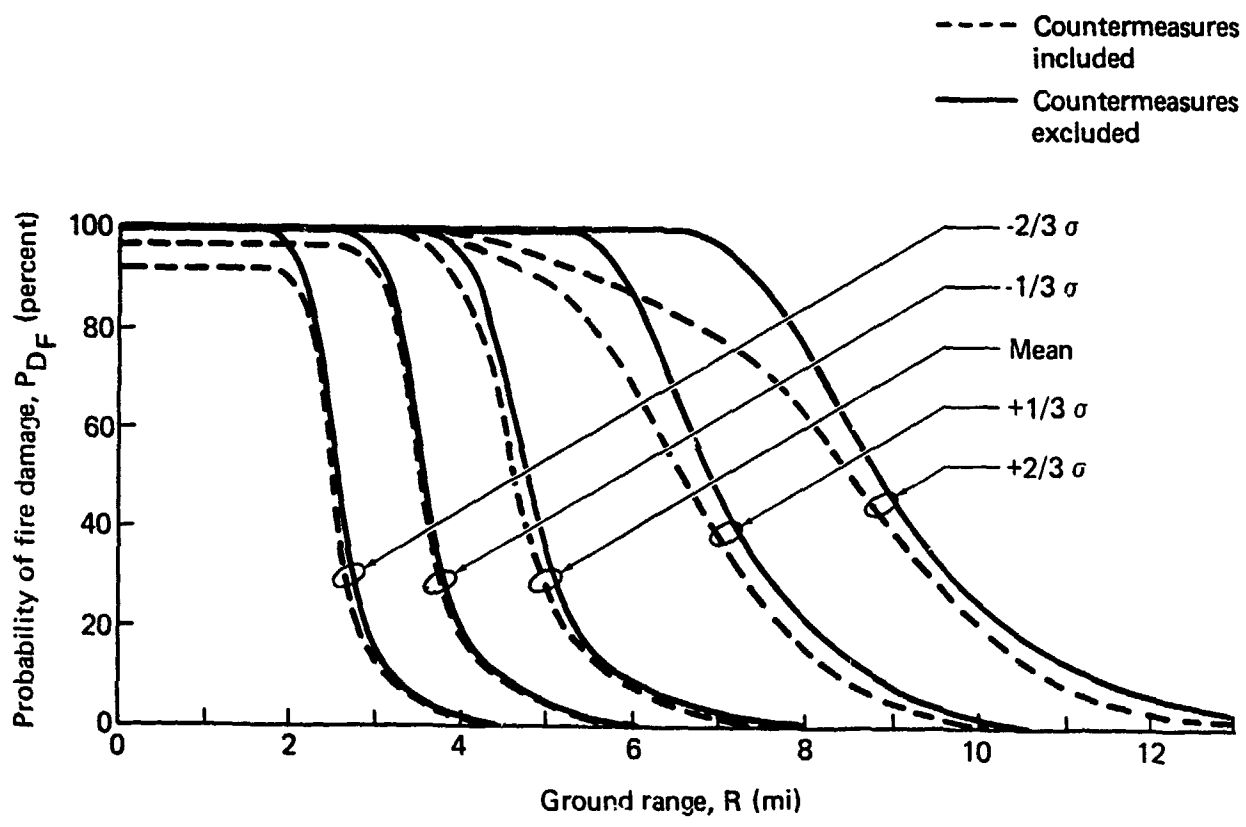


Figure 23. Fire damage range for thermally induced ignitions: combined-parameter variations with and without countermeasures, $W = 1$ MT.

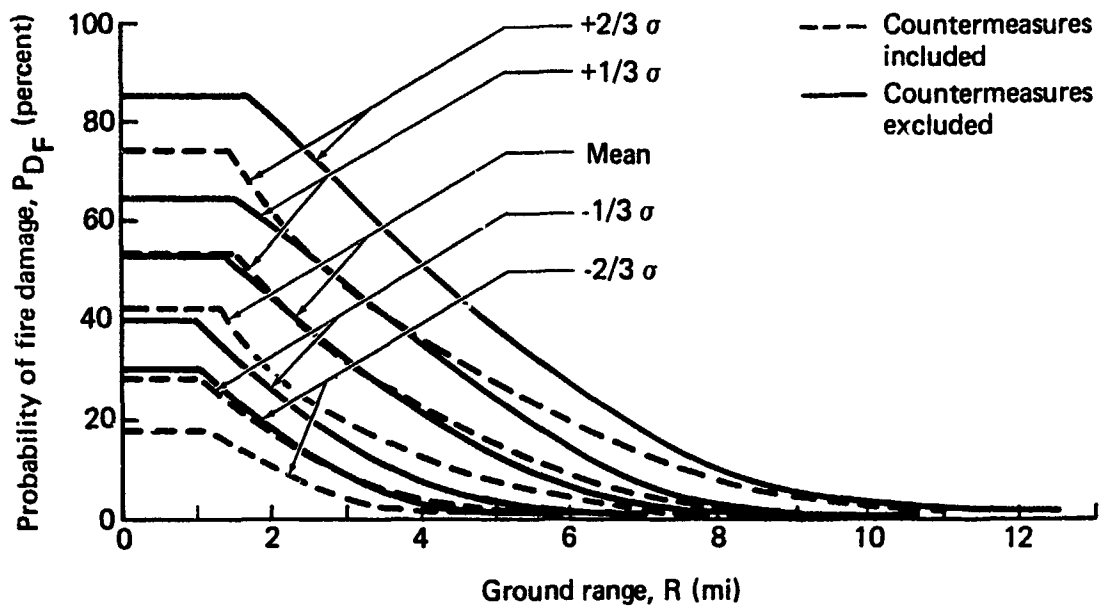


Figure 24. Fire damage range for blast-induced ignitions: combined-parameter variations with and without countermeasures, $W = 50$ KT.

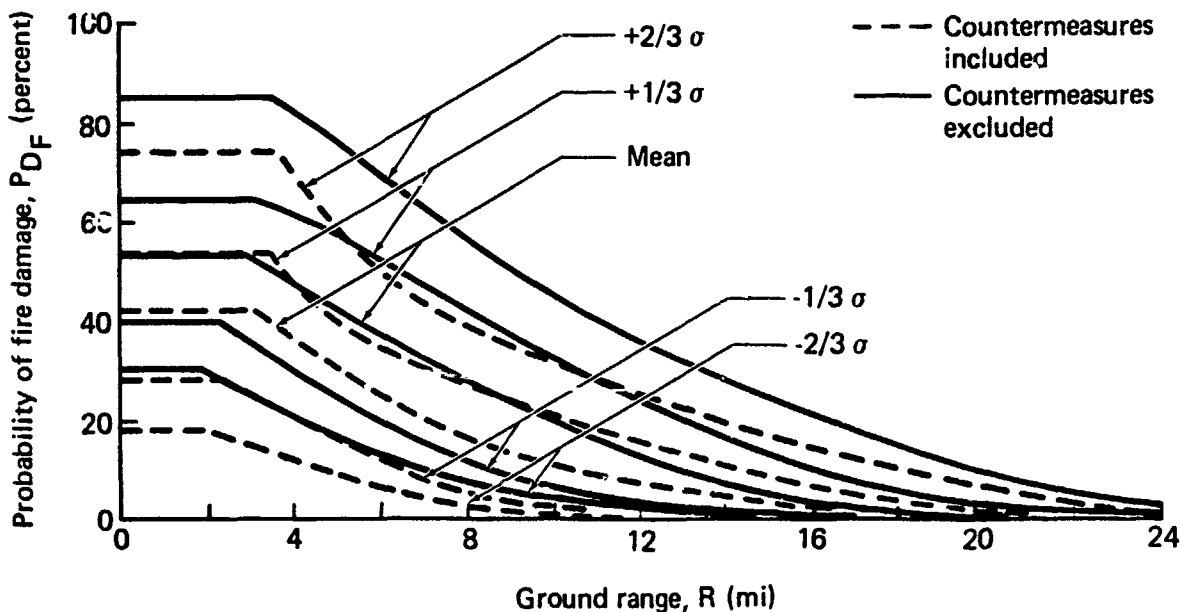


Figure 25. Fire damage range for blast-induced ignitions: combined-parameter variations with and without countermeasures, $W = 1$ MT.

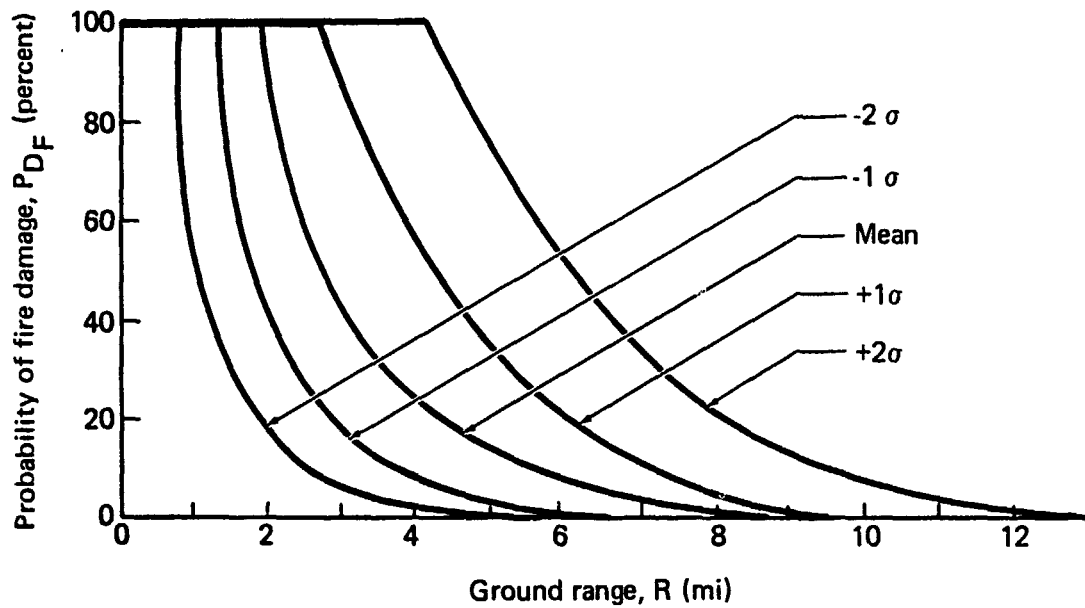


Figure 26. Fire damage range summation curves: all parameters, $W = 50$ KT.

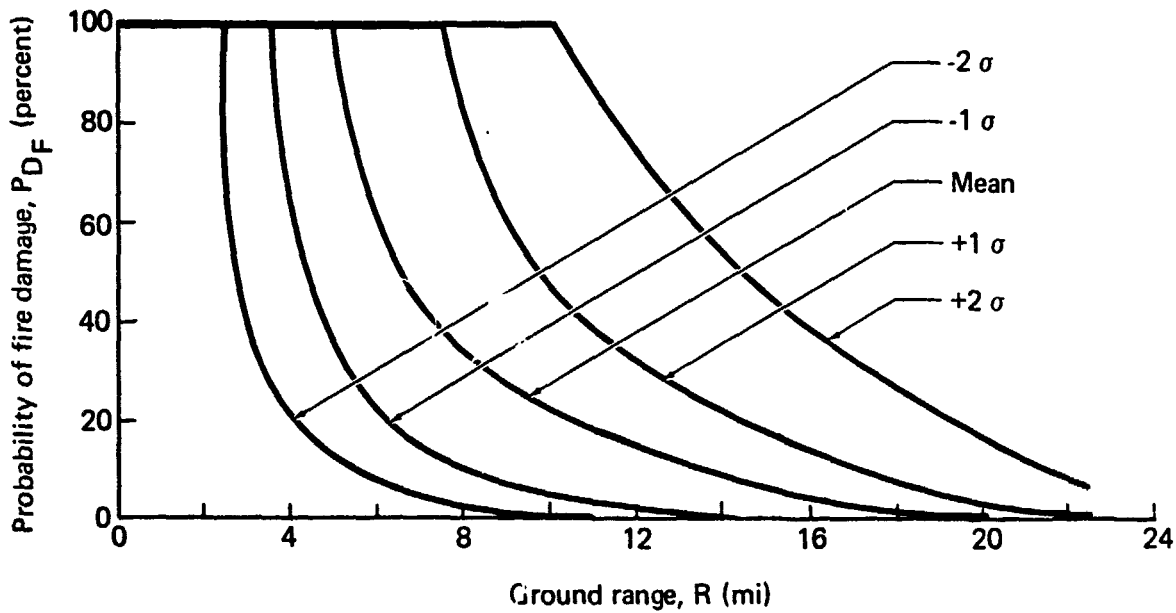


Figure 27. Fire damage range summation curves: all parameters, $W = 1$ MT.

comparable to those presented in Figs. 20 and 21, although are skewed somewhat toward greater damage ranges at the lower probability levels. The wide band of parameter values used to construct the ensemble is reflected in the summation curves. At the 50 percent damage level, the range from -2σ to $+2\sigma$ varies by a factor of 5. The damage range varies by a factor of 2 for the $\pm 1\sigma$ band.

The values selected for each of the independent variables are assumed to represent reasonable parameter choices. The positive standard deviation sets tend toward an expansion of the fire damage range. The negative standard deviation ensembles lead to less damage. In most cases, each parameter variability choice could be improved through research. In constructing the ensembles, rather than assume a specific target, values that may characterize a wide range of targets were considered. Selection of a specific target or urban area should reduce the spread of values characterizing threshold levels, building type/contents indices, and countermeasure effectiveness. Statistical and seasonal definition of target area weather and local environmental conditions would define a narrower range of visibility lengths and probabilities of thermal radiation enhancement or reduction. In any event, the mean, $\pm 1\sigma$, and $\pm 2\sigma$ damage-range curves not only indicate the probable "bonus" damage effect that fire can provide, but the degree of reliability that can be placed on that bonus, and so the potential value of further research to narrow the uncertainties.

SECTION 9
CONCLUSIONS

The fire vulnerability analysis developed in this report has been used to estimate damage ranges based on the target vulnerabilities to fire starts, the immediate weapon effect-target interaction, and the later time fire development. Modifications due to weather conditions, civil defense measures, and uncertainties or variations in atmospheric transmission and target vulnerabilities were considered. Mean and standard deviation fire-damage-range curves were presented for two weapon yields. The results provide a measure of expected fire damage ranges. In general, fire damage radii exceed those for moderate blast damage.

Despite the uncertainties, fire damage can be predicted with useful consistency; such predictions could become as reliable as corresponding blast damage predictions. The inclusion of fire in the damage prediction methodology would improve and extend current damage assessments. In addition to greater damage radii, fire may cause more complete and permanent damage. A structure only moderately damaged by blast may be gutted and rendered useless by fire. Similarly, building contents may survive the blast but be destroyed by the fires.

Some improvements and new directions might be pursued to further develop such a fire-damage-prediction method. Variables not explicitly considered in this study include blast-flame interactions, target shielding by adjacent buildings or topographical features, variable city construction and vulnerabilities, fire breaks, and multiple-burst effects such as target shielding by dust and smoke. Many of these effects, though potentially important, may provide only modest changes in the overall damage prediction. A fire damage model applicable for multiple-weapon attacks is needed.

A fire damage prediction must be based to some extent on the target structure vulnerability. A simplified method might involve a classification system that relates the target vulnerability to burst characteristics such as the total thermal flux or the blast pressure or impulse.

One possibility might be to alter the VN target designation to include the probability of fire damage. Such a revision would be operationally convenient. Alternatively, an added vulnerability designation (FVN) specifically for fire damage probability could be generated for each target. This evaluation would weigh such additional factors as the ignition susceptibility of the structure and contents, the likelihood of blast-induced fire starts, and the proximity of other equally or more susceptible structures from which the fire might spread. Such added considerations would require more computation in arriving at weapon application plans, but potentially may reduce the number and yield of weapons required to achieve specified damage levels or improve estimates of their effectiveness.

The VN system was constructed some three decades ago when both weapons and targets were fewer, smaller, and simpler. The system is well established, but increasingly complex for modern weapon allocation alternatives. Long computer runs are often involved. Although most targets and all cities are vulnerable to fire damage, these vulnerabilities are not now included in the VN system or in damage considerations. The effects of a nuclear attack are thus understated.

The vagarious nature of and lack of specifics in declared national objectives in the use of strategic forces make comprehensive damage evaluation difficult. Both blast and fire will damage targets, but fire will often go farther and cause more complete damage.

A new damage methodology including fire effects need not wait for changes in national objectives. If "moderate damage" to "steel frame" buildings is the appropriate guide for destroying a city of a million or more inhabitants, then fire can only complete the job more effectively. Recent concerns for the adequacy of current criteria and for the consequent choices of overpressure levels and burst heights could be relieved or removed by the inclusion of fire damage.

REFERENCES

- Bond, H. (ed.), *Fire and the Air War*, 1st ed., National Fire Protection Association, Boston, Massachusetts, 1951.
- Brode, H. L., *A Review of Nuclear Explosion Phenomena Pertinent to Protective Construction*, The Rand Corporation, Santa Monica, California, R-425-PR, May 1964.
- , *Analytic Approximations to the Nuclear Blast Wave*, Pacific-Sierra Research Corporation, Note 529, August 1983 (subsequently published as Vol. 12 of PSR Report 1317 and DNA-TR-82-179, 1 June 1983).
- Defense Nuclear Agency (DNA), *Capabilities of Nuclear Weapons*, Parts I and II, DNA Effects Manual No. 1 (NATO Version) [DNA EM-1(N)], Washington, D.C., 1 November 1974.
- Drake, M., Science Applications, Inc., La Jolla, California, private communication, July 1982.
- Fullwood, R. R., and M. W. Tobriner, *Meteorological Environment in the Soviet Union*, Defense Nuclear Agency, Washington, D.C., DNA 3066T, January 1973.
- Gibbons, M. G., *Transmissivity of the Atmosphere for Thermal Radiation from Nuclear Weapons*, U.S. Naval Radiological Laboratory, San Francisco, USNRDL-TR-1060, August 1966.
- Glasstone, S., and P. J. Dolan (eds.), *The Effects of Nuclear Weapons*, 3d ed., U.S. Department of Defense and U.S. Department of Energy (USGPO), Washington, D.C., 1977.
- Larson, D. A., and R. D. Small, *Analysis of the Large Urban Fire Environment, Part I: Theory*, Pacific-Sierra Research Corporation, Report 1210, July 1982a.
- , *Analysis of the Large Urban Fire Environment, Part II: Parametric Analysis and Model City Simulations*, Pacific-Sierra Research Corporation, Report 1210, November 1982b.
- McAuliffe, J., and K. Moll, *Secondary Ignitions in Nuclear Attack*, SRI International, Menlo Park, California, SRI Project 5106, July 1965.
- Martin, S. B., and R. S. Alger (eds.), *Blast/Fire Interactions--Asilomar Conference, April 1981*, SRI International, Menlo Park, California, PYU 3110, August 1981.

REFERENCES (concluded)

Pyne, S. J., *Fire in America*, Princeton University Press, Princeton, New Jersey, 1982.

Sanderlin, J. C., J. A. Ball, and G. A. Johanson, *Mass Fire Model Concept*, Defense Nuclear Agency, Washington, D.C., DNA 5803F, May 1981 (submitted by Mission Research Corporation, Santa Barbara, California).

Small, R. D., and H. L. Brode, "Thermal Radiation from a Nuclear Weapon Burst," *Proceedings of the 1983 Asilomar Conference*, May 1983.

Speicher, S. J., and H. L. Brode, *An Analytic Approximation for Peak Overpressure versus Burst Height and Ground Range over an Ideal Surface*, Pacific-Sierra Research Corporation, Note 336, September 1980.

-----, *Airblast Overpressure Analytic Expression for Burst Height, Range, and Time--over an Ideal Surface*, Pacific-Sierra Research Corporation, Note 385, April 1981 (subsequently published as Chap. VIII of PSR Report 1241 and DNA-TR-81-218, 1 December 1981).

Wilton, C., D. Myronuk, and J. Zaccor, *Secondary Fire Analysis*, Scientific Services, Redwood City, California, Report 8048-6, September 1981.

DISTRIBUTION LIST

DEPARTMENT OF DEFENSE

Asst to the Secretary of Defense, Atomic Energy
ATTN: J. Rubell

Commander in Chief, Atlantic
ATTN: J22
ATTN: J7

Defense Intelligence Agency
ATTN: DB-4C, J. Burfening
ATTN: DB-4C, Rsch. Phys Vuln Br
ATTN: DB-4C2, C. Wiehle
ATTN: RTS-2B
ATTN: S. Halperson

Defense Nuclear Agency
ATTN: SPSS, G. Ullrich
ATTN: SPSS, R. Sweddock
4 cy ATTN: STTI/CA

Defense Technical Info Center
12 cy ATTN: DD

Field Command
Defense Nuclear Agency
ATTN: FCTT, W. Summa
ATTN: FCTXE

Joint Strat Tgt Planning Staff
ATTN: JLK, DNA Rep
ATTN: JLKC
ATTN: JLKS
ATTN: JPPFM
ATTN: JPST

Under Secy of Def for Rsch & Engrg
ATTN: Strat & Theater Nuc For, B. Stephan

DEPARTMENT OF THE ARMY

US Army Engr Waterways Exper Station
ATTN: J. Balsara
ATTN: WESS, S. Kieger

US Army Nuclear & Chemical Agency
ATTN: MONA-OPS, B. Thomas
ATTN: MONA-OPS, J. Kelley

DEPARTMENT OF THE AIR FORCE

Air Force Weapons Laboratory
ATTN: NTE, M. Plamondon
ATTN: NTEd, E. Seusy

Ballistic Missile Office
ATTN: ENSN

Foreign Technology Division
ATTN: SDBF, J. Vent

Strategic Air Command
ATTN: DOCSO
ATTN: DOM
ATTN: NRI/STINFO
ATTN: XPFR
ATTN: XPFS

OTHER GOVERNMENT AGENCIES

US Department of State
ATTN: PM/STM

Central Intelligence Agency
ATTN: OWI, J. Kecoski

DEPARTMENT OF DEFENSE CONTRACTORS

Aerospace Corp
ATTN: J. Crawford
ATTN: L. Seizer
ATTN: R. Eaton

Applied Research Associates, Inc
ATTN: J. Bratton

Applied Research Associates, Inc
ATTN: D. Piepenburg

Applied Research Associates, Inc
ATTN: R. Frank

California Research & Technology, Inc
ATTN: K. Krayenhagen

California Research & Technology, Inc
ATTN: F. Sauer

EG&G Wash Analytical Svcs Ctr, Inc
ATTN: Library

Electro-Mech Systems, Inc
ATTN: R. Shunk

H&H Consultants, Inc
ATTN: J. Haltiwanger
ATTN: W. Hall

JAYCOR
ATTN: E. Wenaas
3 cy ATTN: Library

Kaman Sciences Corp
ATTN: E. Conrad

Kaman Tempo
ATTN: DASIAc

Kaman Tempo
ATTN: DASIAc

Karagozian and Case
ATTN: J. Karagozian

Lockheed Missiles & Space Co, Inc
ATTN: J. Weisner

Pacific-Sierra Research Corp
2 cy ATTN: H. Brode, Chairman SAGE
2 cy ATTN: R. Small

R&D Associates
ATTN: G. Ganong

DEPARTMENT OF DEFENSE CONTRACTORS (Continued)

R&D Associates

ATTN: C. Lee
ATTN: C. Knowles
ATTN: D. Simons
ATTN: J. Lewis
ATTN: P. Haas

Rand Corp

ATTN: P. Davis

Rand Corp

ATTN: B. Bennett

S-CUBED

ATTN: K. Pyatt

DEPARTMENT OF DEFENSE CONTRACTORS (Continued)

TRW Electronics & Defense Sector

ATTN: A. Feldman
ATTN: N. Lipner

Weidinger Assoc, Consulting Engrg

ATTN: T. Deevy

Weidinger Assoc, Consulting Engrg

ATTN: M. Baron

Weidinger Assoc, Consulting Engrg

ATTN: J. Isenberg